PharmOmics: A Species- and Tissue-specific Drug Signature Database and Online Tool for Drug Repurposing

Yen-Wei Chen[1,2,6], Graciel Diamante[1,2,6], Jessica Ding[1,3,6], Thien Xuan Nghiem[1], Jessica Yang[1], Sung-min Ha[1], Peter Cohn[1], Douglas Arneson[1,4], Montgomery Blencowe[1,3], Jennifer Garcia[2], Nima Zaghari[2], Paul Patel[2], and Xia Yang[1,2,3,4,5 *]

[1]Department of Integrative Biology and Physiology, University of California, Los Angeles, CA

[2]Interdepartmental Program of Molecular Toxicology, University of California, Los Angeles, Los Angeles, CA

[3]Interdepartmental Program of Molecular, Cellular, & Integrative Physiology, Los Angeles, Los Angeles, CA

[4] Interdepartmental Program of Bioinformatics, University of California, Los Angeles, Los Angeles, CA

[5]Institute for Quantitative and Computational Biosciences, University of California, Los Angeles, CA

[6]These authors contributed equally.

Correspondence:

*Xia Yang, Ph.D.

Dept. Integrative Biology and Physiology, UCLA

Email: xyang123@ucla.edu

Abstract

Drug development has been hampered by a high failure rate in clinical trials due to efficacy or safety issues not predicted by preclinical studies in model systems. A key contributor is our incomplete understanding of drug functions across organ systems and species. Therefore, elucidating species- and tissue-specific actions of drugs can provide systems level insights into therapeutic efficacy, potential adverse effects, and interspecies differences that are necessary for more effective translational medicine. Here, we present a comprehensive drug knowledgebase and analytical tool, PharmOmics, comprised of genomic footprints of drugs in individual tissues from human, mouse, and rat transcriptome data from GEO, ArrayExpress, TG-GATEs, and DrugMatrix. Using multi-species and multi-tissue gene expression signatures as molecular indicators of drug functions, we developed gene network-based approaches for drug repositioning. We demonstrate the potential of PharmOmics to predict drugs for new disease indications and validated two predicted drugs for non-alcoholic fatty liver disease in mice. We also examined the potential of PharmOmics to identify drugs related to hepatoxicity and nephrotoxicity. By combining tissue- and species-specific *in vivo* drug signatures with biological networks, PharmOmics serves as a complementary tool to support drug characterization.

Key words: PharmOmics, network medicine, tissue specificity, cross-species comparison, drug repositioning, adverse drug reactions, drug toxicity

Background

Drug development has been challenging and costly over the past decades due to the high failure rate in clinical trials (1). Most drugs with excellent efficacy and safety profiles in preclinical studies often encounter suboptimal efficacy or safety concerns in humans (2). This translational gap is likely attributable to our incomplete understanding of the systems level activities of drugs in individual tissues and organ systems (3) as well as the differences between humans and model systems (4).

Drug activities can be captured by gene expression patterns, commonly referred to as gene signatures. By measuring how a pharmacological agent affects the gene signature of a cell or tissue type in a particular species, we can infer the cell- or tissue-specific biological pathways involved in therapeutic processes or toxicological responses. This concept has prompted drug repositioning studies and provided important predictions for repurposing approved drugs for new disease indications (5–10). Similarly, gene signatures can reveal mechanisms underlying adverse drug reactions (ADRs) and be leveraged to predict ADRs as previously shown for liver and kidney toxicity (11–13).

A drug may affect different molecular processes between tissues, providing treatment effects in the desired target tissue(s) but causing toxicity or ADRs in other tissues. Therefore, tissue-specific drug signatures will offer a more systematic understanding of drug actions *in vivo*. In addition, rodent models have been commonly used in toxicology and preclinical studies, yet species-specific effects of drugs have been observed (14) and underlie the lack of efficacy or unexpected ADRs of certain drugs when used in humans (15). Therefore, understanding the species-specific molecular effects of drugs is of high biological importance. A detailed species- and tissue-specific drug genomic signature database will significantly improve our understanding of the molecular networks affected by drugs and facilitate network-based drug discovery and ADR prediction for translational medicine.

The potential of using gene signatures to facilitate target and toxicity identification has led to several major efforts in characterizing genomic signatures related to drug treatment (8,16–18). However, none of the existing platforms offer comprehensive cross-tissue and cross-species *in vivo* assessments of drug activities to allow predictions of drug effects on individual tissues and to help assess the translational potential of a drug based on consistencies or discrepancies between species. For instance, the comparative toxicogenomics database (CTD), a literature-based resource curating chemical-to-gene/protein associations as well as chemical-to-disease

and gene/protein-to-disease connections (16), lacks the cellular and tissue context of the curated interactions. More systematic, data-driven databases like CMAP (8) and LINC1000 (17) focus on characterizing and cataloging the genomic footprints of more than ten thousand chemicals using *in vitro* cell lines (primarily cancer cell lines) to offer global views of molecular responses to drugs in individual cellular systems. However, these *in vitro* cell-line based gene signatures may not always capture *in vivo* tissue-specificity of drug activities. To move into *in vivo* systems, large toxicogenomics databases like TG-GATEs (19) and DrugMatrix from the National Toxicology Programs of the National Institute of Environmental Health Sciences (https://ntp.niehs.nih.gov/drugmatrix/index.html) have become available to provide unbiased transcriptome assessment for heart, muscle, liver, and kidney systems. However, information about other organ systems is limited. Efforts to analyze publicly deposited transcriptomic datasets in GEO (20) and ArrayExpress (21), which have broader tissue coverage, for individual drugs have been described (18), but systematic annotation and integration of species- and tissue-specific effects of drugs have not been achieved.

Here, we present a database that contains 13,382 rat, human, and mouse transcriptomic datasets across >20 tissues covering 941 drugs. We evaluated the tissue- and species-specificity of drug signatures as well as the performance of these signatures in gene network-based drug repositioning, toxicity prediction, target identification, and comparisons of molecular activities between tissues and species. The drug signatures are hosted on an interactive web server, PharmOmics, to enable public access to drug signatures and integrative analyses for drug repositioning (http://mergeomics.research.idre.ucla.edu/runpharmomics.php).

Methods

Curation of tissue- and species-specific drug transcriptomic datasets

As illustrated in **Figure 1**, we compiled a list of clinically relevant drugs, including 766 FDA approved drugs from Kyoto Encyclopedia of Genes and Genomes (KEGG) (16), which overlapped with drugs from the US Food and Drug Administration (FDA), European Medical Agency, and Japanese Pharmaceuticals and Medical Devices Agency, with an additional 175 chemicals from TG-GATEs (19) and DrugMatrix (https://ntp.niehs.nih.gov/drugmatrix/index.html). The compiled drug list was queried against GEO, ArrayExpress, TG-GATEs, and DrugMatrix to identify datasets as of January 2018. Duplicated datasets between data repositories were removed. We developed a semi-

116 automated pipeline combining automated search with manual checking to identify relevant
117 datasets for drug treatment. The automated process first extracts datasets containing drug
118 generic names or abbreviations and then inspects the potential datasets for availability of both
119 drug treatment and control labels in the constituent samples. We also manually checked the
120 recorded labels identified by the automated process to validate the labels and remove
121 potential false detections. Only datasets with n>=3/group in both drug treatment and control
122 groups were included in our downstream analyses. Although a larger sample size is desired,
123 the majority (78.7%) of drug transcriptome datasets have n=3/group, 20.9% datasets have
124 n=2/group, and <1% datasets have n>3/group (**Supplementary Table 1**).
125
126 ***Obtaining drug treatment signatures stratified by species and tissues***
127 Species and tissue labels were retrieved based on the metadata of each dataset. Tissue names
128 were standardized based on the Brenda Tissue Ontology (22). We implemented a search
129 procedure to climb the ontology tree structure to determine the suitable tissue annotations.
130 This was done by first building a priority list of widely used tissues/organs in toxicological
131 research using the Brenda Tissue Ontology tree system. Tissue/organ priority order was set to
132 "kidney", "liver", "pancreas", "breast", "ovary", "adipose tissue", "cardiovascular system",
133 "nervous system", "respiratory system", "urogenital system", "immune system",
134 "hematopoietic system", "skeletal system", "integument" (endothelial and skin tissue),
135 "connective tissue", "muscular system", "gland", "gastrointestinal system", and "viscus"
136 (other non-classified tissue). Tissue terms relevant to each of these tissues or organs were
137 curated from the ontology tree into a tissue/organ ontology table. Next, we looked up terms
138 from our tissue/organ ontology table in the Cell/Organ/Tissue column of the metadata in each
139 transcriptomic dataset. If a tissue/organ term was not found, we searched the title and
140 summary columns of the metadata as well to retrieve additional information. When the search
141 returned multiple tissue terms (for example, breast cancer cell line may be categorized as
142 both epithelial and breast organ), we used the term with the highest priority as described
143 above. We prioritized the tissue terms based on the relevance to toxicology to make tissue
144 assignments unique for each dataset to reduce ambiguity. Manual checking was conducted to
145 confirm the tissue annotation for each dataset.
146
147 For each gene expression dataset, normalized data were retrieved, and quantile distribution of
148 the values were assessed. When a dataset was not normally distributed, log2-transformation
149 using GEO2R (20) was applied. To identify differentially expressed genes (DEGs)
150 representing drug signatures, two different strategies were used. First, the widely used DEG

151 analysis method LIMMA (23) was applied to obtain dose and time segregated signatures
152 under FDR < 0.05. To overcome the low sample size issue and obtain "consensus" drug
153 signatures for a drug/chemical, LIMMA was also applied to datasets where multiple doses
154 and treatment durations were tested, and treatment effect were derived by combining
155 dose/time experiments for the same drug/chemical in each study. Second, we leveraged
156 different studies for the same drugs or chemicals in the same tissue and species to derive
157 meta-analysis signatures. To address heterogeneity in study design, platforms, sample size,
158 and normalization methods across different data repositories, we applied the characteristic
159 direction method from the GeoDE package (24) to derive consistent DEGs for each drug
160 across different data sources. GeoDE was designed to accommodate heterogenous datasets
161 that have differing parameters and outputs between treatment and control groups. It uses a
162 "characteristic direction" measure to identify biologically relevant genes and pathways. The
163 normalized characteristic directions for all genes were then transformed into a non-parametric
164 rank representation. Subsequently, gene ranks of a particular drug from the same tissue/organ
165 system and the same organism were aggregated across datasets using the Robust Rank
166 Aggregation method (25), a statistically controlled process to identify drug DEGs within each
167 tissue for each species. Robust Rank Aggregation provides a non-parametric meta-analysis
168 across different ranked lists to obtain commonly shared genes across datasets, which avoids
169 statistical issues associated with heterogeneous datasets. It computes a null distribution based
170 on randomized gene ranks and then compares the null distribution with the empirical gene
171 ranks to obtain a p-value for each gene. The robust rank aggregation process was done for the
172 upregulated and downregulated genes separately to obtain DEGs for both directions under
173 Bonferroni-adjusted p-value < 0.01, a cutoff implemented in the Robust Rank Aggregation
174 algorithm. To obtain species-level signatures for each drug, we further aggregated DEGs
175 across different organs tested for each drug within each species.
176
177 Pathway analysis of individual drug signatures was conducted using Enrichr (26) by
178 intersecting each signature with pathways or gene sets from KEGG (27) and gene ontology
179 biological process (GOBP) terms (28). In addition, pathway enrichment analysis based on
180 network topology analysis (29) was conducted using ROntoTools (30). Pathways at false
181 discovery rate (FDR) < 0.05 were considered significant in both methods.
182
183 We curated 14,366 drug signatures segregated by treatment dosage and duration, tissue, and
184 species, covering 719 drugs and chemicals, among which 544 are FDA approved. In addition,
185 our meta signatures is a consensus of 4,349 signatures covering 551 drugs across treatment

regimens. In total, the entire database is based on 13,382 rat, human, and mouse transcriptomic datasets across >20 tissue or organ systems across 941 drugs and chemicals from GEO, ArrayExpress, DrugMatrix, and TG-GATEs to derive drug signatures. These rat, human, and mouse datasets cover >20 tissue or organ systems. The toxicogenomics databases TG-GATEs and DrugMatrix mainly contain liver and kidney datasets from rats, while public data repositories GEO and ArrayExpress contain datasets with broader tissue and species coverage (**Figure 2A**). Overall, the rat datasets are mainly from liver and kidney whereas human and mouse datasets also contained signatures from other tissues and organs such as breast and the nervous system (**Figure 2B**). There is also a species bias between the data repositories; GEO covered more mouse and human datasets, TG-GATEs mainly has human and rat datasets, and DrugMatrix curated more rat datasets (**Figure 2C)**.

Comparison of PharmOmics with existing drug signature platforms

To assess the degree of agreement in drug signatures between the PharmOmics database and existing platforms, we compared PharmOmics with the CREEDS (18) and L1000FWD (31) databases, for which drug signatures are accessible **(Supplementary methods)**. As shown in **Supplementary Figure 1**, both the PharmOmics dose/time-segregated signatures and the meta signatures showed better concordance with the two existing platforms than the agreement between CREEDS and L1000FWD, as reflected by higher overlap fold enrichment score and lower statistical p values. The three platforms have differences in the datasets and analytical strategies and therefore are complementary. Due to the lack of full access to CMAP signatures, we were not able to systematically compare PharmOmics against CMAP.

Web server implementation of PharmOmics

To allow easy data access and use of PharmOmics, we have created a freely accessible web tool deployed on the same Apache server used to host Mergeomics (32), a computational pipeline for integrative analysis of multi-omics datasets to derive disease-associated pathways, networks, and network regulators (http://mergeomics.research.idre.ucla.edu).

The PharmOmics web server features three functions (**Figure 3**). First, it allows queries for species- and tissue-stratified drug signatures and pathways for both the dose/time-segregated and meta signatures. Details of statistical methods (e.g, LIMMA vs characteristic direction), signature type (dose/time-segregated vs meta), and datasets used are annotated. The drug query also includes a function for DEG and pathway signature comparisons between user-

selected species and tissues which can be visualized and downloaded. Second, it features a network drug repositioning tool that is based on the connectivity of drug signatures in PharmOmics to user input genes such as a disease signature. This tool requires a list of genes and a gene network that can be chosen from our preloaded gene regulatory networks if relevant or a custom upload (see Applications below for details in implementation). In the output, Z-score and p-value results of network repositioning are displayed and available for download. In addition, we list the overlapping genes between drug signatures in the given network and the input genes, the drug genes with direct connections to input genes through one-edge extension, and input genes with one-edge connections to drug genes in the downloadable results file. The output page also provides network visualization which details the genes affected by a drug and their overlap with and direct connections to user input genes using Cytoscape.js. The network nodes and edges files are also available for download and can be used on Cytoscape Desktop. **Figure 4** shows the web interface of the input submission form (**Figure 4A**) and results display of the network repositioning tool using a sample liver network and a sample hyperlipidemia gene set (**Figure 4B**). Lastly, the web server offers a gene overlap-based drug repositioning tool that assesses direct overlap between drug gene signatures and user input genes. Gene overlap-based drug repositioning requires a single list of genes or separate lists of upregulated and downregulated genes and outputs the Jaccard score, odds ratio, Fisher's exact test p-value, within-species rank, and gene overlaps for drugs showing matching genes with the input genes. This gene overlap-based approach is similar to what was implemented in other drug repositioning tools, but the network-based repositioning approach is unique to PharmOmics.

Experimental methods for NAFLD drug validation

Seven-week old C57BL/6 male mice were purchased from the Jackson Laboratory (Bar Harbor, ME). After acclimation the animals were randomly assigned to four experimental groups (n=7-9/group) on different diets/treatments: regular chow diet (Control) (Lab Rodent Diet 5053, St. Louis, MO), high fat high sucrose (HFHS) diet (Research Diets-D12266B, New Brunswick, NJ) to induce hepatic steatosis, a key NAFLD phenotype, HFHS diet with fluvastatin treatment (NAFLD + Flu), and HFHS diet with aspirin treatment (NAFLD + Asp). The target intake concentrations of fluvastatin and aspirin were 15mg/kg and 80 mg/kg, respectively, which were chosen based on doses used in previous studies that did not show toxicity (33,34). These experimental diets were then administered for 10 weeks. The average fluvastatin intake was 14.98 mg/kg/day, and the average aspirin intake was 79.67 mg/kg/day.

During drug treatment, metabolic phenotypes such as body weight, body fat and lean mass composition were monitored weekly. Fat and lean mass were measured with Nuclear Magnetic Resonance (NMR) Bruker minispec series mq10 machine (Bruker BioSpin, Freemont, CA). For metabolic phenotypes measured at multiple time points (body weight gain and adiposity), differences between groups were analyzed using a 2-way ANOVA followed by Sidak's multiple comparisons test. At the end of treatment, livers from all groups were weighed, flash frozen, and stored at −80 °C until lipid analysis. Hepatic lipids were extracted using the Folch method as previously described (35). The lipid extracts were analyzed by the UCLA GTM Mouse Transfer Core for triglyceride (TG), total cholesterol (TC), unesterified cholesterol (UC), and phospholipids (PL) levels by colorimetric assay from Sigma (St. Louis, MO) according to the manufacturer's instructions. All animal experiments were approved by the UCLA Animal Research Committee.

Results

Evaluating the ability of PharmOmics to extract drug targets and target pathways

It remains unclear whether drug DEGs reflect drug targets. To evaluate this possibility, we retrieved known targets for the drugs included in PharmOmics from the DrugBank database (36) and used three different methods to evaluate the potential of DEGs for drug target identification. The first method assessed direct gene overlaps between known drug targets and DEG signatures. The second assessed overlaps between known drug target pathways and drug DEG pathways from pathway enrichment analysis. The last method was based on whether known drug targets were within the close neighborhood of drug DEGs in molecular networks, including the STRING network (37) and tissue-specific Bayesian networks (BNs) **(Supplementary methods)**. For drugs with multiple dose and time regimens, only the signature with the best performance was used in these analyses.

The drug target recovery rates using PharmOmics drug DEGs for gene overlap, pathway overlap, STRING network overlap, and liver BN overlap with liver DEGs were 22%, 59.1%, 41.7%, and 60.2%, respectively, and were significantly higher than the rates using random genes (**Supplementary Table 2)**. Although these rates are low, gene overlap drug target recovery rate using PharmOmics signatures was higher than using CMAP (14%) and L1000 (17%) signatures, and drug target recovery was improved by pathway and network approaches. Notably, matching the tissue between DEGs and network improved the target detection rate. However, we note that while the pathway- and network-based approaches

increased the detection rate for true drug targets, the number of false positives was also increased. Overall, our results show that although PharmOmics has certain value in drug target and pathway retrieval as shown by better performance than random genes and other platforms, the retrieval rate is low. These results suggest that DEGs do not recover direct drug targets well but more likely reflect target-related pathways, and caution should be taken when using DEGs for target identification.

Utility of PharmOmics drug signatures in retrieving known therapeutic drugs for various diseases

We next evaluate the ability of PharmOmics drug signatures to identify drugs for diseases based on overlaps or network connectivity in gene signatures matched by tissue. We hypothesized that if a drug is useful for treating a disease, the drug signatures and disease signatures likely target similar pathways and therefore have direct gene overlaps or connect extensively in gene networks. For gene overlap-based drug repositioning, we calculate the Jaccard score, gene overlap fold enrichment, and Fisher's exact test p values as the overlap measurements. For network-based drug repositioning, we used a network proximity measurement between drug and diseases genes which was previously applied to protein interaction networks and known drug targets (5) **(Supplementary methods)**. Here, we used tissue-specific BNs and tested the mean shortest distance between drug DEGs and disease genes.

The performance of PharmOmics drug repositioning was assessed using hyperlipidemia as the first test case, as multiple known drugs are available as positive controls. Since hyperlipidemia is most relevant to LDL and liver tissue, we retrieved LDL causal genes and pathways in liver tissue based on LDL GWAS and liver genetic regulation of gene expression using Mergeomics (**Supplementary methods**) (38), a method that can extract causal genes, pathways, and networks for diseases (39,40). In addition to retrieving disease genes from GWAS, a hyperlipidemia signature from CTD (16) was also used as an alternative source. For each drug with different dose and treatment durations, the signature with the highest overlap with the disease signature was used to represent the drug. Gene overlap- and network-based methods using dose/time-segregated signatures had similar overall performance (~90% AUC) in identification of antihyperlipidemic drugs (**Figure 5A, 5B)**, and the dose/time-segregated signatures performed better than the meta signatures when using network-based repositioning (**Figure 5C-5D)**. When compared to other platforms, PharmOmics was able to retrieve higher prediction rankings for the known drugs (**Table 1**)

and better AUC (**Figure 5C-5D)** than CMAP and L1000 and higher balanced accuracy (**Supplementary Table 3**) than CREEDS, CMAP, and L1000. These results support the capacity of the PharmOmics platform as a drug repositioning tool.

We also examined the network overlap patterns of the top drugs consistently retrieved by the PharmOmics platform, lovastatin (ranked top 1% in both PharmOmics and CREEDS) and oxymetholone (ranked top 1% in PharmOmics and ranked as 15% in CREEDS). Both drugs targeted lipid metabolism genes (e.g. *Sqle* and *Hmgcr*) and PPAR pathways in the hyperlipidemia network (**Figure 5E, 5F**), but more lovastatin DEGs connected to disease genes compared to oxymetholone DEGs. These results support the utility of a network-based drug repositioning approach that does not require the direct retrieval of a known drug target or direct overlap of drug DEGs with disease genes.

We further evaluated the performance of PharmOmics in retrieving known drugs for other diseases. Using CTD disease signatures for hyperuricemia, we found network-based repositioning obtained 90% AUC (p=0.009) for detection of anti-hyperuricemia drugs, whereas the gene overlap-based method did not yield a significant AUC (prediction ranks in **Supplementary Table 4**). We also queried hepatitis signatures and achieved 83% AUC (p< 0.001) using the network method and 79% AUC (p<0.001) using the gene overlap method in retrieving non-steroid anti-inflammatory agents **(**prediction ranks in **Supplementary Table 5)**. Finally, using diabetes signatures, PharmOmics was able to predict PPAR gamma agonist drugs (79% AUC, p=0.04), but not sulfonylurea drugs which act on the pancreatic islet to enhance insulin release (prediction ranks in **Supplementary Table 6**). We note that the paucity of drug signatures in diabetes relevant tissues/cells such as the islets and the digestive system likely explains why sulfonylurea drugs are harder to retrieve. Overall, these various test cases using known therapeutic drugs as positive controls support the utility of network-based drug repositioning for select diseases when drug signatures from the appropriate tissues are used.

Use of PharmOmics to predict drugs for NAFLD

After establishing the performance of PharmOmics in drug repositioning using the case studies above, we applied PharmOmics to predict potential drugs for NAFLD, for which there is currently no approved drugs. Using NAFLD steatosis signatures from a published study (40) and the CTD database (16), we predicted PPAR alpha agonists (clofibrate, fenofibrate, bezafibrate, and gemfibrozil), HMG-CoA reductase inhibitors (lovastatin,

fluvastatin, and simvastatin), and a PPAR gamma agonist (rosiglitazone) among the top 10% of the drug candidates (**Supplementary Table 7**). PPAR agonists have been supported as potential drugs for NAFLD (41–52). Statins have shown efficacy in animal models (34,53), although clinical results are controversial (54,55). Additional predicted drugs included aspirin, which was recently reported to be associated with reducing liver fibrosis progression (56).

In vivo validation of drug repositioning predictions for NAFLD

Next, we sought to experimentally validate the ability of two top ranked drugs by PharmOmics, fluvastatin and aspirin, to mitigate liver steatosis as predicted by PharmOmics and assess the accuracy of repositioning ranks. Compared to other platforms (**Supplementary Table 7**), fluvastatin was ranked high consistently in PharmOmics (top 5%), CMAP (top 1% in all cells combined, 20% in HEPG2), CREEDS (20%), and L1000 (top 1% in all cells combined, 55% in HEPG2). In comparison, aspirin was ranked higher in PharmOmics (top 5%) compared to CREEDS (30%) and CMAP (35%) and was not documented in L1000. Therefore, these predictions are relatively unique to PharmOmics.

Comparison between the mice in HFHS group (NAFLD) and the chow group (Control) confirmed HFHS induced NAFLD phenotypes including increased body weight, adiposity, and hepatic steatosis (**Supplementary Figure 2A and 2B**). Comparison of the fluvastatin and aspirin treated groups with the NAFLD group revealed significant drug effects on body weight gain for both fluvastatin ($p<0.0001$; **Figure 6A**) and aspirin ($p<0.0001$; **Figure 6B**). The adiposity phenotype (fat and lean mass ratio) also showed significant drug effects from both fluvastatin ($p<0.0001$; **Figure 6C**) and aspirin ($p=0.0157$; **Figure 6D**).

There was no significant difference in total liver weight among the groups (**Supplementary Figure 2C** for Control and NAFLD group comparison; **Supplementary Figure 3A and 3B** for NAFLD and drug group comparisons). As expected, the HFHS group had significantly elevated levels of liver TG compared to controls, without changes in other lipids measured such as TC, UC, and PL (**Supplementary Figure 2D**). In the drug treatment groups, both fluvastatin ($p=0.0044$) and aspirin ($p=0.0023$) induced significant decreases in hepatic TG compared to the NAFLD group, without any effect on TC, UC, and PL (**Figure 5E-5F**).

We further investigated whether the effects of the drugs on NAFLD phenotypes were confounded by food and water intake. No effect of food intake was observed in the NAFLD + Flu group; however, there was a significant decrease in food intake in the NAFLD + Asp

group (**Supplementary Figure 3C-3D**). No effect on water intake was found for both groups (**Supplementary Figure 3E-3F**). We next adjusted for food intake in the NAFLD phenotypic analysis for body weight gain, adiposity, and TG levels using linear regression. After the adjustment, the significant effects of fluvastatin on NAFLD phenotypes remained (body weight gain p=0.0306; adiposity p=0.0022; hepatic TG p=0.0190). For aspirin, the significant effects on adiposity (p=0.0479) and hepatic TG (p=0.0372) remained, but the effect on body weight gain was no longer significant (p=0.0559). Overall, food/water intake did not have major influence on treatment effects on NAFLD observed for both drugs.

Our experimental validation experiments support the efficacy of both fluvastatin and aspirin in mitigating NAFLD. The effects of fluvastatin were stronger than that of aspirin and visualization of the network overlaps between NAFLD signatures and drug signatures revealed more extensive disease network connections for fluvastatin than for aspirin (**Figure 6G-6H**), supporting their repositioning ranks and potential mechanisms of action. The signatures of the two drugs connected to pathways involved in NAFLD such as PPAR signaling pathways, fatty acid and steroid biosynthesis (**Figure 6G-6H**).

Utility of PharmOmics drug signatures in predicting and understanding hepatotoxicity

We further explored the potential of coupling PharmOmics drug signatures and tissue networks to predict liver toxicity, a major type of ADR for which both toxicity signatures and orthogonal ADR documentations from various independent databases are available for performance evaluation. We used the chemical-induced liver injury signature containing 435 genes from CTD to match with PharmOmics drug signatures through liver gene networks. We then used both the histological severity from TG-GATEs and the independent FDA drug-induced liver disease (DILI) categories ("most", "less" – moderate/mild DILI adverse reactions compared to the "most" category, and "no" DILI concern) as *in silico* independent validation of the drugs predicted by PharmOmics that match with the CTD liver toxicity signature.

First, we examined the relationship between the matching scores of PharmOmics signatures and the histological severity grading based on TG-GATEs. Both the network-based and gene overlap-based scores from PharmOmics increased with higher histological severity defined by TG-GATEs (**Figure 7A**). Next, we examined the dose-dependent effects across the TG-GATEs histological severity categories as well as the three FDA DILI categories. Our results indicated that severe histological grading occurred mainly at higher drug doses within both

the "less" and "most" DILI concern categories (**Figure 7B**). Analysis of the relationship between dose/time-segregated signatures and network-based PharmOmics scores indicated that drug treatment at higher doses had higher network matching ranks in PharmOmics and more severe DILI (**Figure 7C**). In addition, we tested the performance of PharmOmics in predicting hepatotoxic drugs from the FDA DILI drug database. PharmOmics dose/time-segregated signatures resulted in higher performance (67% AUC) compared to the meta signatures (60% AUC) and the other platforms tested such as CREEDS, CMAP, and L1000 (AUC 50-53%; **Figure 7D; Supplementary Figure 4**). Top drug predictions based on the complete hepatotoxicity signatures were wy-14643 (experimental drug with severe histological finding in TG-GATEs), dexamethasone (moderate DILI concern category in FDA and moderate histological finding in TG-GATEs), phenobarbital (moderate DILI concern), indomethacin ("most" DILI concern), and fenofibrate (moderate DILI concern).

Since CTD curated a large number of genes (435 genes) related to chemical induced liver injury, we hypothesized that this large network could be divided into subnetworks indicative of different mechanisms towards liver toxicity, which could improve toxicity prediction for drugs with different mechanisms. We first examined network overlapping patterns of the top 5 predicted drugs by using the CTD liver injury genes (**Figure 7E**) and found consistent targeting of gene subnetworks across top predictions. We then applied the Louvain clustering method to divide the liver injury network into subnetworks and filtered subnetworks with less than 10 genes to reduce uncertainty. These different subnetworks showed varying abilities in identifying drugs with DILI concerns (**Supplementary Table 8**). The best performing subnetwork showed improved AUC compared to the whole network (75% vs 67%; **Figure 7D**). Further scrutinization of key genes documented in CTD signatures of the top performing subnetwork revealed that the antioxidant gene *GSR*, the phase 2 drug metabolizer *NAT2*, and the inflammatory response gene *IRAK1* showed the best predictability (**Supplementary Table 8**). These results suggest that the network-based toxicity prediction approach may help prioritize predictive genes, pathways, and subnetworks related to hepatotoxicity.

Utility of PharmOmics drug signatures in predicting and understanding nephrotoxicity

We also examined the performance of PharmOmics in predicting nephrotoxicity, another ADR for which both toxicity signature and drug ADR documentations are available from independent sources to help validate performance.

Nephrotoxicity signatures were curated from CTD using either the chronic kidney disease signature (CKD, 56 genes) or acute kidney injury signature (AKI, 120 genes), which were matched with PharmOmics drug signatures to predict drugs matching CKD or AKI signatures. The PharmOmics predictions were then validated using kidney histological severity documented by TG-GATEs or nephrotoxicity defined by DrugBank. There were 13 shared genes between CKD and AKI signatures including several inflammatory factors *TNF*, *TGFB1*, *NFKB1*, and *IL6*. We found that unlike AKI signatures, using CKD signatures against PharmOmics drug signatures resulted in network matching scores (not gene overlap scores) that agreed well with histological severity documented in TG-GATEs (**Figure 8A**). Therefore, we focused on using CKD signatures in downstream network-based analyses. We found that PharmOmics drug signatures of higher doses predicted more drugs with severe or moderate kidney histology categorized by TG-GATEs as well as drugs with nephrotoxicity as defined by DrugBank (**Figure 8B**). However, when examining the relationship between PharmOmics network scores across doses and DrugBank nephrotoxicity categories (non-nephrotoxic or nephrotoxic), the network scores did not show a significant dose-dependent relationship (**Figure 8C**). This is in contrast to the dose-dependent relationship observed for hepatotoxicity analysis (**Figure 7C**). The weaker performance of PharmOmics in nephrotoxicity prediction could be due to the smaller number of kidney drug datasets (~1k) compared to liver drug datasets (~5k) based on data availability.

Finally, we assessed the performance of PharmOmics and other tools in identifying DrugBank nephrotoxic agents. PharmOmics dose/time-segregated (64% AUC, p=0.001) and meta databases (61% AUC, p=0.028) both showed a significant performance (**Figure 8D**), whereas from the other tools evaluated only CMAP (63% AUC, p<0.001) showed a significant performance (L1000 43% and CREEDS 56% AUC, non-significant). The top 5 nephrotoxic drugs predicted by PharmOmics were dexamethasone (potential CKD alleviating agent) (57,58), naproxen (documented nephrotoxic drug in DrugBank), cholecalciferol (potential CKD alleviating agent) (59), beta-estradiol (potential alleviating agent in women) (60,61), and ibuprofen (documented nephrotoxic drug in DrugBank). We also examined the gene overlap patterns of the top drugs with the CKD gene network (**Figure 8E**) and found sparse overlap, which again is in contrast to the top hepatotoxicity drugs (**Figure 7E**).

Overall, our assessment of the application of PharmOmics in toxicity or ADR prediction supports its potential value but also emphasizes that PharmOmics drug signatures may have differing performance in different use cases. Several factors, including the toxicity signatures

used (e.g., CKD signature performed better than AKI signature for nephrotoxicity prediction), ADR/toxicity annotation (e.g., TG-GATEs or DrugBank), and signature matching method (network-based approach better than gene overlap approach) can all significantly affect the results. We also note that our network approach does not differentiate toxicity-inducing drugs from toxicity-mitigating drugs since it is based on network connectivity and not the directionality of gene signatures.

Utility of meta-analysis signatures to understand tissue and species specificity

We used meta signatures, which reflect the dose-independent, consistent genes affected by drugs across studies in the same tissue or species, to evaluate tissue and species specificity of drugs by analyzing the overlap in gene signatures for each drug across different tissues and species and visualized the results using UpSetR (62). As shown in **Figure 9A**, the overlap rate in the DEGs of the same drug between tissues and organs is usually less than 5%, indicating a high variability in DEGs between tissues. As an example, we examined atorvastatin, a HMGCR (β-Hydroxy β-methylglutaryl-CoA receptor) inhibitor, which has well understood mechanisms and has been broadly tested in different tissues under the human species label. We found that two DEGs (*TSC22D3, THBS1*) were shared across tissues (**Figure 9B**). These genes are involved in extracellular matrix and inflammation, suggesting these processes are common targets of atorvastatin across tissues. Among the pathways shared across tissues, immune related pathways were shared between blood cells and liver cells but not in prostate cells from the urogenital system (**Figure 9C, Supplementary Table 9)**. Pathway analysis indicated that steroid synthesis and drug metabolism pathways were altered primarily in liver, which is expected as the known target of statin drugs is HMGCR, the rate limiting enzyme in cholesterol biosynthesis in liver. Blood monocyte DEGs indicated changes in inflammation related pathways, while GPCR ligand binding proteins were altered in prostate cancer cells. The tissue specificity of drug meta signatures revealed through our analysis supports tissue-specific therapeutic responses and side effects and emphasizes the need for comprehensive inclusion of drug signatures from different tissue systems as implemented in the PharmOmics framework.

We also found evidence for high species specificity. As shown in **Figure 9D**, the pair-wise overlaps in DEGs between species for the same drug is generally lower than 5%. Here we chose PPAR gamma receptor agonist rosiglitazone as an example because this drug has datasets across human, rat, and mouse in PharmOmics, and its mode of actions is well-studied. As shown in **Figure 9E** and **9F**, nine genes (*CPT1C, AKR1B1, VNN1, ACSM3,*

CD36, CPT1A, PDK4, ZNF669, ADH1C) and several pathways (PPAR signaling and fatty acid, triacylglycerol, and ketone body metabolism) were consistently identified from liver DEGs across species (**Supplementary Table 10**), reflecting the major species-independent pharmacological effects of rosiglitazone. Bile acid related genes were altered in rat datasets, whereas retinol metabolism and adipocytokine pathways were altered in human datasets. The species-specific differences identified highlight the importance of understanding the physiological differences among model systems to facilitate drug design with better translational potential. Our cross-species comparative studies also emphasize the need to investigate drugs in multiple species, as only 21% of the unique drug-tissue pairs (236 out of 1144) from PharmOmics meta signatures have data from two or more species.

Discussion

Here we present PharmOmics, a publicly available drug signature database along with an open-access web interface for accessing and utilizing the signatures for various applications. PharmOmics utilizes published drug-related transcriptomic datasets across multiple data repositories and provides unique tissue-, species-, and dose/time-stratified gene signatures that are more reflective of *in vivo* activities of drugs. We also developed a unique framework for drug repositioning based on tissue-specific gene network models. We examined the potential applications of PharmOmics for various utilities including drug repurposing, toxicity prediction, target identification, and comparisons of molecular activities between tissues and species. We also carried out *in silico* performance assessments across drug signature databases and *in vivo* mouse experiments to validate our network-based drug predictions for NAFLD.

Compared to the well-established CMAP and LINC1000 platforms, PharmOmics focuses more on *in vivo* settings and likely captures more physiologically relevant drug signatures to improve drug repositioning performance. Compared to a previous crowdsourcing effort which also utilizes publicly available drug datasets (18), our PharmOmics platform included more curated databases (TGGATEs + drugMatrix Affymetrix + drugMatrix Codelink datasets compared to only drugMatrix Codelink datasets from CREEDS) and involved systematic tissue, species, and treatment regimen stratification to facilitate drug repositioning. Our platform is also the only tool utilizing a gene network framework rather than direct gene overlap approach.

The use of tissue annotation with Brenda Tissue Ontology helps normalize organ labels and improves comparability of datasets. The unique tissue- and species-specific analyses implemented in PharmOmics allows for comprehensive molecular insight into the actions of drug molecules in individual tissues and species. Our results support that different species have unique drug responses in addition to shared features; therefore, drug responses obtained in animal models require caution when translating to humans. This notion agrees with the long-observed high failure rate of drug development that has primarily relied on preclinical animal models and argues for greater consideration and understanding of inter-species differences in drug actions.

In addition to tissue and species stratification, we also provide detailed dose/time-segregated drug signatures, which can help better understand the dose- and time-dependent effects of drugs through gene signature and pathway comparisons offered through our web server. By contrast, the meta-analysis signatures capture the consistent genes and pathways across treatment regimens, which likely represent core, dose/time-independent mechanisms, and help address the sample size issue of individual datasets since the majority of drug treatment datasets have n<=3/group. Dose/time-segregated signatures performed better than meta signatures for both drug repositioning and toxicity prediction. However, meta signatures showed better performance than CMAP, LINC1000, and CREEDs **(Figure 5, 7, 8)**, and can also significantly shorten the computation time in network-based repositioning applications. For instance, computation using 1251 human meta signatures can be completed in 40 minutes, whereas using ~14,000 dose/time-segregated signatures can take 4 hours. These estimates will vary depending on input data size and server load.

Previous drug repositioning studies support the utility of a protein network-based approach for drug repositioning. Here we show that combining the drug transcriptomic signatures in PharmOmics with tissue-specific gene regulatory networks and gene signatures of diseases can retrieve known therapeutic drugs, predict potential therapeutic avenues, and predict tissue toxicity. Compared to other platforms, the use of tissue- and species-specific drug signatures along with network biology is a unique strength of PharmOmics, which enables drug prioritization based on network proximity rather than direct gene overlaps. We demonstrate in various applications that network-based analysis had a superior performance to that of gene overlap-based analysis. Moreover, the tissue-specific network connections between drugs and diseases or toxicity offer molecular and mechanistic insights into the therapeutic or toxic effects of drugs. For instance, fluvastatin showed different NAFLD overlapping

patterns compared to aspirin, which inferred differences in disease repositioning depending on different drug mechanisms.

In general, gene signatures of drugs reflect cascades of downstream events after drug administration. The initial drug target(s) may or may not be captured by drug DEGs due to the lack of dynamic information in the DEGs. Therefore, we explored if PharmOmics signatures as well as signatures from other platforms can be used to retrieve drug targets through integration with pathway or network information. Our results show that DEGs may help inform on the pathways affected by the drugs but retrieving the direct targets can be difficult. We caution the use of drug DEGs from any drug signature platform for direct target identification.

There are several limitations in this study. First, our computational pipeline may not be able to identify all of the drug datasets from GEO and ArrayExpress database. Variations in annotations of drug names, sample size, definition of treatment vs control groups, and tissue/cell line labeling across datasets make it challenging to design a fully automated pipeline to curate drug signatures. It is therefore crucial for GEO and ArrayExpress repositories to offer clear definitions and instructions for metadata generation in order to standardize terms across datasets to facilitate future data reuse. Secondly, the coverage of tissue, species, and treatment regimens across drugs is unbalanced, preventing a thorough comparison across tissues, species, dosages, and treatment windows. We will continue to refine the pipeline and update our PharmOmics database periodically to include more datasets as they become available to increase the coverage of datasets and drug signatures. Thirdly, the sample sizes for drug treatment studies tend to be small (majority with n=3/group or less), which limit the statistical power and reliability of the drug signatures when individual studies were analyzed. This is an intrinsic limitation of existing drug studies and highlights the need for systematic efforts to increase sample sizes in such studies. To mitigate this concern and reduce the reliance on individual studies, we implemented a meta-analysis strategy to aggregate drug signatures from individual studies and derive meta signatures. However, this strategy removes dosage- and time-dependent effects. We offer both options in our database to mitigate sample size concerns through meta-analysis and retain dose and time regimen information through dose/time-segregated analysis. Fourth, our network-based applications are currently limited in the coverage of high-quality tissue specific regulatory networks and computational power. We will continue to expand and improve the tissue networks and computing environment in our web server. Lastly,

639 systematic validation efforts are needed to substantiate the value of our platform. We utilized
640 both *in silico* performance assessments and *in vivo* experiments to validate our predictions in
641 limited settings. We mainly focused on liver related diseases with well-documented drugs
642 and disease signatures (hyperlipidemia, hyperuricemia, diabetes, and liver/kidney toxicity) to
643 benchmark the utilities of PharmOmics and experimentally validated two drugs predicted for
644 NAFLD. As with the other existing platforms such as CMAP and LINC1000, future
645 application studies and community-based validation efforts are necessary to assess the value
646 of PharmOmics.
647

648 ## Conclusion

649 We have established a new drug signature database, PharmOmics, across different species
650 and tissues, which captures the systems level *in vivo* activities of drug molecules. In addition,
651 we demonstrate the possible means to integrate these signatures with network biology to
652 address drug repositioning needs for disease treatment and to predict and characterize liver
653 and kidney injury. PharmOmics has the potential to complement other available drug
654 signature databases to accelerate drug development and toxicology research. Our
655 PharmOmics database and pipeline will be updated periodically to include newly available
656 datasets to increase the coverage of the drug signatures across tissues and species. It should
657 be noted that we aim to position PharmOmics as a data-driven compensatory tool in
658 hypothesis generation. Integration with known drug characteristics to select drug candidates
659 and design follow up experiments are still essential.
660

661 ## List of abbreviations

662	ADR	adverse drug reactions
663	CTD	comparative toxicogenomics database
664	KEGG	Kyoto Encyclopedia of Genes and Genomes
665	DEG	differential expressed genes
666	FDR	false discovery rate
667	wKDA	weighted key driver analysis
668	NAFLD	non-alcoholic fatty liver disease
669	LDL	low-density lipoprotein cholesterol
670	GWAS	genome-wide association study
671	BN	Bayesian gene regulatory network
672	ROC	Receiver operating characteristic
673	HMGCR	β-Hydroxy β-methylglutaryl-CoA receptor

PPAR	Peroxisome proliferator-activated receptor
GPCR	G-protein coupled receptor

Declaration

Ethics approval and consent to participate

Not applicable.

Consent for publication

Not applicable.

Availability of data and materials

Indexed dataset catalog, pre-computed gene signatures and pre-computed pathway enrichments for individual drugs are deposited to and accessible through the PharmOmics web server (http://mergeomics.research.idre.ucla.edu/runpharmomics.php). We also implemented functions for same-tissue between-species comparison and same-species between-tissue comparison. Direct download of select drug signatures is also enabled. In addition, network-based drug repositioning analysis and gene overlap-based drug repositioning analysis using all drug signatures are available at http://mergeomics.research.idre.ucla.edu/runpharmomics.php.

Competing interests

The authors declare that they have no competing interests.

Funding

YC was supported by UCLA Eureka fellowship and Burroughs Wellcome Fund Inter-school Training Program in Chronic Diseases. DA was supported by NIH-NCI National Cancer Institute (T32CA201160), UCLA dissertation year fellowship and UCLA Hyde fellowship. XY was funded by NIH DK104363 and DK117850. GD was supported by the National Institute of Environmental Health Sciences (T32ES015457) and the American Diabetes Association Postdoctoral Fellowship (1-19-PDF-007-R).

Authors' contributions

YC curated and analyzed data, constructed database, and designed and conducted application studies. GD, JY, and PC conducted validation experiments. JD, TXN, DH, and MB designed and implemented the PharmOmics web server. DA provided support in data curation and analysis. GA, JG, NZ, and PP assisted with data curation. YC, GD, JD, and XY wrote the manuscript. XY designed and supervised the research. All authors contributed to manuscript editing.

Acknowledgements

We thank Dr. Patrick Allard at UCLA for constructive input on the manuscript. We thank Dr. Avi Ma'ayan at Icahn School of Medicine at Mount Sinai for providing L1000FWD and CREEDS data for comparison.

References:

1. Morgan S, Grootendorst P, Lexchin J, Cunningham C, Greyson D. The cost of drug development: a systematic review. Health Policy. 2011 Apr;100(1):4–17.
2. Yu HWH. Bridging the translational gap: collaborative drug development and dispelling the stigma of commercialization. Drug Discov Today. 2016;21(2):299–305.
3. Lin Z, Will Y. Evaluation of Drugs With Specific Organ Toxicities in Organ-Specific Cell Lines. Toxicol Sci. 2011 Dec;126(1):114–27.
4. Denayer T, Stöhr T, Van Roy M. Animal models in translational medicine: Validation and prediction. New Horizons Transl Med. 2014;2(1):5–11.
5. Cheng F, Desai RJ, Handy DE, Wang R, Schneeweiss S, Barabási A-L, et al. Network-based approach to prediction and population-based validation of in silico drug repurposing. Nat Commun [Internet]. 2018;9:2691. Available from: http://www.ncbi.nlm.nih.gov/pmc/articles/PMC6043492/
6. Guney E, Menche J, Vidal M, Barábasi A-L. Network-based in silico drug efficacy screening. Nat Commun [Internet]. 2016;7:10331. Available from: http://www.ncbi.nlm.nih.gov/pmc/articles/PMC4740350/
7. Barabasi AL, Gulbahce N, Loscalzo J. Network medicine: a network-based approach to human disease. Nat Rev Genet. 2010/12/18. 2011;12(1):56–68.
8. Subramanian A, Narayan R, Corsello SM, Peck DD, Natoli TE, Lu X, et al. A Next Generation Connectivity Map: L1000 Platform and the First 1,000,000 Profiles. Cell. 2017/12/02. 2017;171(6):1437-1452.e17.
9. Hall CJ, Wicker SM, Chien A-T, Tromp A, Lawrence LM, Sun X, et al. Repositioning drugs for inflammatory disease – fishing for new anti-inflammatory agents. Dis Model & Mech [Internet]. 2014;7(9):1069. Available from: http://dmm.biologists.org/content/7/9/1069.abstract
10. Corbett A, Pickett J, Burns A, Corcoran J, Dunnett SB, Edison P, et al. Drug repositioning for Alzheimer's disease. Nat Rev Drug Discov [Internet]. 2012;11:833. Available from: http://dx.doi.org/10.1038/nrd3869
11. Godoy P, Bolt HM. Toxicogenomic-based approaches predicting liver toxicity in vitro. Arch Toxicol [Internet]. 2012;86(8):1163–4. Available from: https://doi.org/10.1007/s00204-012-0892-5
12. Low Y, Uehara T, Minowa Y, Yamada H, Ohno Y, Urushidani T, et al. Predicting

Drug-Induced Hepatotoxicity Using QSAR and Toxicogenomics Approaches. Chem Res Toxicol [Internet]. 2011;24(8):1251–62. Available from: https://doi.org/10.1021/tx200148a

13. AbdulHameed MD, Ippolito DL, Stallings JD, Wallqvist A. Mining kidney toxicogenomic data by using gene co-expression modules. BMC Genomics. 2016/10/12. 2016;17(1):790.

14. Toutain P-L, Ferran A, Bousquet-Melou A. Species differences in pharmacokinetics and pharmacodynamics. Handb Exp Pharmacol. 2010;(199):19–48.

15. Wong CH, Siah KW, Lo AW. Estimation of clinical trial success rates and related parameters. 2018 Jan;

16. Davis AP, Grondin CJ, Johnson RJ, Sciaky D, King BL, McMorran R, et al. The Comparative Toxicogenomics Database: update 2017. Nucleic Acids Res [Internet]. 2017;45(Database issue):D972–8. Available from: http://www.ncbi.nlm.nih.gov/pmc/articles/PMC5210612/

17. Wang Z, Clark NR, Ma'ayan A. Drug-induced adverse events prediction with the LINCS L1000 data. Bioinformatics [Internet]. 2016;32(15):2338–45. Available from: http://dx.doi.org/10.1093/bioinformatics/btw168

18. Wang Z, Monteiro CD, Jagodnik KM, Fernandez NF, Gundersen GW, Rouillard AD, et al. Extraction and analysis of signatures from the Gene Expression Omnibus by the crowd. Nat Commun [Internet]. 2016;7:12846. Available from: http://dx.doi.org/10.1038/ncomms12846

19. Igarashi Y, Nakatsu N, Yamashita T, Ono A, Ohno Y, Urushidani T, et al. Open TG-GATEs: a large-scale toxicogenomics database. Nucleic Acids Res. 2014/10/15. 2015;43(Database issue):D921-7.

20. Barrett T, Wilhite SE, Ledoux P, Evangelista C, Kim IF, Tomashevsky M, et al. NCBI GEO: archive for functional genomics data sets—update. Nucleic Acids Res [Internet]. 2013;41(D1):D991–5. Available from: http://dx.doi.org/10.1093/nar/gks1193

21. Kolesnikov N, Hastings E, Keays M, Melnichuk O, Tang YA, Williams E, et al. ArrayExpress update—simplifying data submissions. Nucleic Acids Res [Internet]. 2015;43(D1):D1113–6. Available from: http://dx.doi.org/10.1093/nar/gku1057

22. Gremse M, Chang A, Schomburg I, Grote A, Scheer M, Ebeling C, et al. The BRENDA Tissue Ontology (BTO): the first all-integrating ontology of all organisms for enzyme sources. Nucleic Acids Res [Internet]. 2011;39(Database issue):D507–13. Available from: http://www.ncbi.nlm.nih.gov/pmc/articles/PMC3013802/

23. Ritchie ME, Phipson B, Wu D, Hu Y, Law CW, Shi W, et al. limma powers

778 differential expression analyses for RNA-sequencing and microarray studies. Nucleic
779 Acids Res. 2015 Apr;43(7):e47–e47.
780 24. Clark NR, Hu KS, Feldmann AS, Kou Y, Chen EY, Duan Q, et al. The characteristic
781 direction: a geometrical approach to identify differentially expressed genes. BMC
782 Bioinformatics [Internet]. 2014;15:79. Available from:
783 https://www.ncbi.nlm.nih.gov/pubmed/24650281
784 25. Kolde R, Laur S, Adler P, Vilo J. Robust rank aggregation for gene list integration and
785 meta-analysis. Bioinformatics [Internet]. 2012;28(4):573–80. Available from:
786 https://www.ncbi.nlm.nih.gov/pubmed/22247279
787 26. Kuleshov M V, Jones MR, Rouillard AD, Fernandez NF, Duan Q, Wang Z, et al.
788 Enrichr: a comprehensive gene set enrichment analysis web server 2016 update.
789 Nucleic Acids Res [Internet]. 2016;44(Web Server issue):W90–7. Available from:
790 http://www.ncbi.nlm.nih.gov/pmc/articles/PMC4987924/
791 27. Kanehisa M, Furumichi M, Tanabe M, Sato Y, Morishima K. KEGG: new
792 perspectives on genomes, pathways, diseases and drugs. Nucleic Acids Res [Internet].
793 2017;45(Database issue):D353–61. Available from:
794 http://www.ncbi.nlm.nih.gov/pmc/articles/PMC5210567/
795 28. Expansion of the Gene Ontology knowledgebase and resources. Nucleic Acids Res.
796 2016/12/03. 2017;45(D1):D331-d338.
797 29. Draghici S, Khatri P, Tarca AL, Amin K, Done A, Voichita C, et al. A systems biology
798 approach for pathway level analysis. Genome Res. 2007/09/04. 2007
799 Oct;17(10):1537–45.
800 30. Voichita C, Ansari S, Draghici S. ROntoTools: R Onto-Tools suite. 2019.
801 31. Wang Z, Lachmann A, Keenan AB, Ma'ayan A. L1000FWD: fireworks visualization
802 of drug-induced transcriptomic signatures. Bioinformatics [Internet]. 2018 Jun
803 15;34(12):2150–2. Available from: http://dx.doi.org/10.1093/bioinformatics/bty060
804 32. Shu L, Zhao Y, Kurt Z, Byars SG, Tukiainen T, Kettunen J, et al. Mergeomics:
805 multidimensional data integration to identify pathogenic perturbations to biological
806 systems. BMC Genomics [Internet]. 2016;17(1):874. Available from:
807 http://www.ncbi.nlm.nih.gov/pubmed/27814671
808 33. Zhu K, Hu M, Yuan B, Liu J-X, Liu Y. Aspirin attenuates spontaneous recurrent
809 seizures in the chronically epileptic mice. Neurol Res. 2017 Aug;39(8):744–57.
810 34. Park HS, Jang JE, Ko MS, Woo SH, Kim BJ, Kim HS, et al. Statins Increase
811 Mitochondrial and Peroxisomal Fatty Acid Oxidation in the Liver and Prevent Non-
812 Alcoholic Steatohepatitis in Mice. Diabetes Metab J. 2016/04/21. 2016 Oct;40(5):376–

813 85.
814 35. FOLCH J, LEES M, SLOANE STANLEY GH. A simple method for the isolation and
815 purification of total lipides from animal tissues. J Biol Chem. 1957 May;226(1):497–
816 509.
817 36. Wishart DS, Feunang YD, Guo AC, Lo EJ, Marcu A, Grant JR, et al. DrugBank 5.0: a
818 major update to the DrugBank database for 2018. Nucleic Acids Res. 2017/11/11.
819 2018;46(D1):D1074-d1082.
820 37. Szklarczyk D, Morris JH, Cook H, Kuhn M, Wyder S, Simonovic M, et al. The
821 STRING database in 2017: quality-controlled protein–protein association networks,
822 made broadly accessible. Nucleic Acids Res [Internet]. 2017;45(Database
823 issue):D362–8. Available from:
824 http://www.ncbi.nlm.nih.gov/pmc/articles/PMC5210637/
825 38. Shu L, Zhao Y, Kurt Z, Byars SG, Tukiainen T, Kettunen J, et al. Mergeomics:
826 multidimensional data integration to identify pathogenic perturbations to biological
827 systems. BMC Genomics [Internet]. 2016;17(1):874. Available from:
828 https://doi.org/10.1186/s12864-016-3198-9
829 39. Shu L, Chan KHK, Zhang G, Huan T, Kurt Z, Zhao Y, et al. Shared genetic regulatory
830 networks for cardiovascular disease and type 2 diabetes in multiple populations of
831 diverse ethnicities in the United States. PLoS Genet. 2017/09/29.
832 2017;13(9):e1007040.
833 40. Chella Krishnan K, Kurt Z, Barrere-Cain R, Sabir S, Das A, Floyd R, et al. Integration
834 of Multi-omics Data from Mouse Diversity Panel Highlights Mitochondrial
835 Dysfunction in Non-alcoholic Fatty Liver Disease. Cell Syst. 2018/01/24.
836 2018;6(1):103-115.e7.
837 41. Liss KHH, Finck BN. PPARs and nonalcoholic fatty liver disease. Biochimie. 2017
838 May;136:65–74.
839 42. Abd El-Haleim EA, Bahgat AK, Saleh S. Resveratrol and fenofibrate ameliorate
840 fructose-induced nonalcoholic steatohepatitis by modulation of genes expression.
841 World J Gastroenterol. 2016 Mar;22(10):2931–48.
842 43. Ratziu V, Charlotte F, Bernhardt C, Giral P, Halbron M, Lenaour G, et al. Long-term
843 efficacy of rosiglitazone in nonalcoholic steatohepatitis: results of the fatty liver
844 improvement by rosiglitazone therapy (FLIRT 2) extension trial. Hepatology. 2010
845 Feb;51(2):445–53.
846 44. Ratziu V, Giral P, Jacqueminet S, Charlotte F, Hartemann-Heurtier A, Serfaty L, et al.
847 Rosiglitazone for nonalcoholic steatohepatitis: one-year results of the randomized

placebo-controlled Fatty Liver Improvement with Rosiglitazone Therapy (FLIRT) Trial. Gastroenterology. 2008 Jul;135(1):100–10.

45. Zhang N, Lu Y, Shen X, Bao Y, Cheng J, Chen L, et al. Fenofibrate treatment attenuated chronic endoplasmic reticulum stress in the liver of nonalcoholic fatty liver disease mice. Pharmacology. 2015;95(3–4):173–80.

46. Laurin J, Lindor KD, Crippin JS, Gossard A, Gores GJ, Ludwig J, et al. Ursodeoxycholic acid or clofibrate in the treatment of non-alcohol-induced steatohepatitis: a pilot study. Hepatology. 1996 Jun;23(6):1464–7.

47. Fernandez-Miranda C, Perez-Carreras M, Colina F, Lopez-Alonso G, Vargas C, Solis-Herruzo JA. A pilot trial of fenofibrate for the treatment of non-alcoholic fatty liver disease. Dig Liver Dis. 2008 Mar;40(3):200–5.

48. Hertz R, Bar-Tana J. Peroxisome proliferator-activated receptor (PPAR) alpha activation and its consequences in humans. Toxicol Lett. 1998 Dec;102–103:85–90.

49. Kawaguchi K, Sakaida I, Tsuchiya M, Omori K, Takami T, Okita K. Pioglitazone prevents hepatic steatosis, fibrosis, and enzyme-altered lesions in rat liver cirrhosis induced by a choline-deficient L-amino acid-defined diet. Biochem Biophys Res Commun. 2004 Feb;315(1):187–95.

50. Nan Y-M, Fu N, Wu W-J, Liang B-L, Wang R-Q, Zhao S-X, et al. Rosiglitazone prevents nutritional fibrosis and steatohepatitis in mice. Scand J Gastroenterol. 2009;44(3):358–65.

51. Neuschwander-Tetri BA, Brunt EM, Wehmeier KR, Oliver D, Bacon BR. Improved nonalcoholic steatohepatitis after 48 weeks of treatment with the PPAR-gamma ligand rosiglitazone. Hepatology. 2003 Oct;38(4):1008–17.

52. Torres DM, Jones FJ, Shaw JC, Williams CD, Ward JA, Harrison SA. Rosiglitazone versus rosiglitazone and metformin versus rosiglitazone and losartan in the treatment of nonalcoholic steatohepatitis in humans: a 12-month randomized, prospective, open-label trial. Hepatology. 2011 Nov;54(5):1631–9.

53. Bravo M, Raurell I, Hide D, Fernández-Iglesias A, Gil M, Barberá A, et al. Restoration of liver sinusoidal cell phenotypes by statins improves portal hypertension and histology in rats with NASH. Sci Rep. 2019;9(1):20183.

54. Pastori D, Polimeni L, Baratta F, Pani A, Del Ben M, Angelico F. The efficacy and safety of statins for the treatment of non-alcoholic fatty liver disease. Dig Liver Dis. 2015;47(1):4–11.

55. Sigler MA, Congdon L, Edwards KL. An Evidence-Based Review of Statin Use in Patients With Nonalcoholic Fatty Liver Disease. Clin Med Insights Gastroenterol.

2018 Jul;11:1179552218787502–1179552218787502.

56. Simon TG, Henson J, Osganian S, Masia R, Chan AT, Chung RT, et al. Daily Aspirin Use Associated With Reduced Risk For Fibrosis Progression In Patients With Nonalcoholic Fatty Liver Disease. Clin Gastroenterol Hepatol. 2019 May;

57. Moonen L, Geryl H, D'Haese PC, Vervaet BA. Short-term dexamethasone treatment transiently, but not permanently, attenuates fibrosis after acute-to-chronic kidney injury. BMC Nephrol. 2018;19(1):343.

58. Tsunoda R, Usui J, Hoshino J, Fujii T, Suzuki S, Takaichi K, et al. Corticosteroids pulse therapy and oral corticosteroids therapy for IgA nephropathy patients with advanced chronic kidney disease: results of a multicenter, large-scale, long-term observational cohort study. BMC Nephrol. 2018 Sep;19(1):222.

59. Westerberg P-A, Sterner G, Ljunggren Ö, Isaksson E, Elvarson F, Dezfoolian H, et al. High doses of cholecalciferol alleviate the progression of hyperparathyroidism in patients with CKD Stages 3–4: results of a 12-week double-blind, randomized, controlled study. Nephrol Dial Transplant. 2018 Mar;33(3):466–71.

60. Mankhey RW, Bhatti F, Maric C. 17β-Estradiol replacement improves renal function and pathology associated with diabetic nephropathy. Am J Physiol Physiol. 2005 Feb;288(2):F399–405.

61. Suzuki H, Kondo K. Chronic kidney disease in postmenopausal women. Hypertens Res. 2012;35(2):142–7.

62. Conway JR, Lex A, Gehlenborg N. UpSetR: an R package for the visualization of intersecting sets and their properties. Bioinformatics [Internet]. 2017;33(18):2938–40. Available from: http://dx.doi.org/10.1093/bioinformatics/btx364

Tables

Table 1. Prediction percentile of FDA approved antihyperlipidemic drug based on hyperlipidemia signatures from MergeOmics (MO) pipeline and CTD database across different platforms tested. HEPG2 results from both L1000 and CMAP were retrieved for tissue specificity comparison.

Platform	**PharmOmics dose/time seg network**		**PharmOmics dose/time seg Jaccard**		**PharmOmics meta**		**CREEDS**		**CMAP**		**CMAP HEPG2**		**L1000**		**L1000 HEPG2**	
Disease gene signature	MO	CTD	MO	CTD	MO	CTD	MO	CTD	MO	CTD	MO	CTD	MO	CTD	MO	CTD
Atorvastatin	0.951	0.794	0.981	0.957	0.498	0.316	0.989	0.82	0.913	0.164	0.414	0.31	0.962	0.668	0.405	0.307
Bezafibrate	0.856	0.995	0.901	0.982	0.981	0.932	0.571	0.95	0.332	0.561	0.439	0.915	0.394	0.755	NA	NA
Cerivastatin	0.989	0.848	0.995	0.962	0.798	0.719	0.986	0.836	0.879	0.516	NA	NA	0.967	0.761	NA	NA
Clofibrate	0.965	0.97	0.802	0.927	0.951	0.992	0.737	0.986	0.196	0.291	0.153	0.433	0.31	0.615	NA	NA
Clofibric acid	0.93	0.58	0.949	0.892	NA	NA	NA	NA	NA	NA	NA	NA	NA	NA	NA	NA
Fenofibrate	0.984	0.986	0.908	0.883	0.954	0.954	0.797	0.943	0.121	0.108	0.229	0.201	NA	NA	NA	NA
Fluvastatin	1	0.997	1.000	0.924	0.97	0.985	1	0.815	0.905	0.963	0.807	0.118	0.958	0.514	0.513	0.327
Gemfibrozil	0.992	0.962	0.984	0.873	0.787	0.844	0.9	0.712	0.677	0.612	NA	NA	0.363	0.591	NA	NA
Lovastatin	0.995	0.984	0.986	0.986	0.905	0.43	0.993	0.632	0.972	0.084	0.528	0.346	0.992	0.979	0.415	0.765
Nafenopin	0.726	0.943	0.472	0.864	NA	NA	0.431	0.712	NA	NA	NA	NA	NA	NA	NA	NA
Niacin	0.192	0.873	0.821	0.309	0.137	0.711	0.719	0.343	0.671	0.171	0.606	0.069	0.107	0.307	NA	NA
Pravastatin	0.894	0.339	0.911	0.862	NA	NA	0.979	0.854	0.829	0.669	0.727	0.934	0.592	0.717	NA	NA
Simvastatin	0.949	0.935	0.856	0.992	0.916	0.909	0.996	0.9	0.972	0.951	0.844	0.573	0.987	0.843	0.595	0.425
Ciprofibrate	NA	NA	NA	NA	NA	NA	NA	NA	0.685	0.998	0.84	0.288	0.292	0.272	NA	NA
Ezetimibe	NA	NA	NA	NA	NA	NA	NA	NA	0.905	0.982	0.514	0.757	0.657	0.269	0.366	0.101
Probucol	NA	NA	NA	NA	NA	NA	NA	NA	0.552	0.115	0.021	0.696	0.018	0.529	NA	NA
Rosuvastatin	NA	NA	NA	NA	NA	NA	NA	NA	0.913	0.056	0.855	0.238	0.905	0.464	NA	NA
Median	**0.951**	**0.943**	**0.911**	**0.924**	**0.911**	**0.876**	**0.94**	**0.828**	**0.829**	**0.516**	**0.528**	**0.346**	**0.624**	**0.603**	**0.415**	**0.327**
Mean	**0.879**	**0.862**	**0.890**	**0.878**	**0.79**	**0.779**	**0.841**	**0.792**	**0.701**	**0.483**	**0.537**	**0.452**	**0.607**	**0.592**	**0.459**	**0.385**

Figure legends

Figure 1. PharmOmics data processing pipeline. FDA approved drugs based on KEGG database were searched against GEO, ArrayExpress, TG-GATEs, and DrugMatrix data repositories. Additional experimental drugs and chemicals from TG-GATEs and DrugMatrix were also included. Only datasets with drug treatment and control samples were retrieved. Datasets were first annotated with tissue and species information, followed by retrieval of dose/time-segregated or meta-analysis drug signatures using two different methods. Dose/time-segregated signatures were retrieved from individual datasets using LIMMA. Meta signatures across datasets of the same drugs were obtained by first applying GeoDE to obtain a ranked gene list for each treatment experiment, followed by meta-analysis using the Robust Rank Aggregation method. These signatures were used to conduct drug repositioning analysis and hepatotoxicity/nephrotoxicity prediction based on direct gene overlaps or a gene network-based approach.

Figure 2. Summary of available datasets based on data sources, tissues, and species. Y-axis indicates unique dataset counts, and X-axis indicates (A) tissue and data resources, (B) tissue and species, and (C) data resources and species.

Figure 3. PharmOmics web server. The web server hosts drug signature and pathway queries, between-tissue and between-species drug signature comparisons, and network-based and gene overlap-based drug repositioning. Users are able to query, download, and perform drug repositioning using all species- and tissue-specific meta and dose/time-segregated signatures. Interactive results tables and network visualizations are displayed on the website and available for download.

Figure 4. User interface of network drug repositioning web tool using sample hyperlipidemia gene set and sample mouse Bayesian gene regulatory network. (A) Inputs to network drug repositioning includes i) signature type to query (meta-analyzed, dose/time-segregated with top 500 genes per signature, or dose/time-segregated with all genes), ii) network (custom upload or select a sample network), iii) species (relating to the species of the network being used), and iv) genes. In this case we choose dose/time-segregated signatures using top 500 genes, a sample liver network, mouse/rat species, and the sample hyperlipidemia gene set (loaded from ‘Add sample genes’). If human gene symbols are provided with the ‘Mouse/Rat’ species selection, the genes will be converted to mouse/rat symbols. (B) After the job is complete, the results file is displayed on the website and

945 available for download. A subset of the drug network containing the drug genes that are first
946 neighbors to input genes and all input genes can be visualized using the "Display Network"
947 button which will load an interactive display of the subnetwork topology. The oxymetholone
948 drug signature in rat liver is a top hit, and the drug network is shown on the right. Additional
949 data in the downloadable results file include the genes that are both a drug gene and an input
950 gene in the network, drug genes that are directly connected (first neighbor) to input genes,
951 and input genes directly connected to drug genes.
952
953 **Figure 5. Drug repositioning for hyperlipidemia**. AUC plots for network-based
954 repositioning and gene overlap-based repositioning in identifying anti-hyperlipidemia drugs
955 against other drugs using (A) Mergeomics hyperlipidemia signature or (B) CTD
956 hyperlipidemia signature. Comparison of drug repositioning performance between
957 PharmOmics network-based approach with CREEDS (using the "combined score" generated
958 by the enrichment analysis tool implemented in Enrichr), L1000, and CMAP query system
959 using (C) Mergeomics hyperlipidemia signature and (D) CTD hyperlipidemia signature. For
960 drugs with multiple datasets with different doses and treatment times, only the best
961 performing signature was used. (E) Drug-disease subnetwork of Mergeomics hyperlipidemia
962 signature (red) and lovastatin signature (blue) showing first neighbor (direct) connections. (F)
963 Drug-disease subnetwork Mergeomics hyperlipidemia signature (red) and oxymetholone
964 signature (blue) showing first neighbor connections. Wilcoxon signed rank test was used to
965 calculate significance between gene overlap/network z-scores between groups. *, **, ***
966 indicates $p < 0.05$, $p < 0.01$ and $p < 0.001$ repectively.
967
968 **Figure 6. *In vivo* validation of predicted drugs Fluvastatin and Aspirin on preventing**
969 **NAFLD phenotypes in C57BL/6J mice.** (A and B) Time course of body weight gain in
970 mice treated with fluvastatin (A) and aspirin (B) over 10 weeks. (C and D) Time course of fat
971 mass and muscle mass ratio (adiposity) in mice treated with fluvastatin (C) and aspirin (D)
972 over 10 weeks. (A-D) Data were analyzed by two-way ANOVA followed by Sidak post-hoc
973 analysis to examine treatment effects at individual time points. P value < 0.05 was considered
974 significant and is denoted by an asterisk (*). (E and F) Quantification of lipids in the liver of
975 mice on fluvastatin (E) and aspirin (F) treatment for 10 weeks. Triglyceride (TG), Total
976 Cholesterol (TC), Unesterified Cholesterol (UC), Phospholipid (PL). (D and E) Data were
977 analyzed using two-sided Student's t-test. P value < 0.05 was considered significant and is
978 denoted by an asterisk (*). Sample size n = 7-9/group. High fat high sucrose (HFHS)
979 group (NAFLD); HFHS with fluvastatin (NAFLD + Flu); HFHS with aspirin (NAFLD +

Asp). (G-H) Gene network view of fluvastatin gene signatures overlapping with NAFLD disease signatures (G) Gene network view of aspirin gene signatures overlapping with NAFLD disease signatures (H).

Figure 7. Utility of PharmOmics drug signatures in hepatotoxicity prediction based on matching between PharmOmics drug signatures and hepatotoxicity signatures of drug induced liver injury (DILI) curated from comparative toxicogenomics database (CTD). (A) Boxplots of Jaccard score-based hepatotoxicity ranking (left) and network-based hepatoxicity ranking (right) by PharmOmics, across four categories of liver injury histological severity defined by the independent TG-GATEs database (x-axis). PharmOmics hepatotoxicity scores are higher for more severe liver injury categories. (B) PharmOmics hepatotoxicity prediction scores based on gene signatures of higher drug doses correspond to more severe liver injury categories defined by TG-GATES across three DILI concern categories ("no", "less", "most") defined by FDA. (C) Boxplots of network-based hepatoxicity scores show increased scores at higher doses across three FDA DILI concern categories. (D) ROC curves comparing PharmOmics with other tools in predicting hepatotoxic drugs from the FDA DILI drug database. For PharmOmics, three sets of tests were performed, where dose/time-segregated drug signatures, meta signatures, or a hepatotoxicity subnetwork was used. (E) Liver hepatotoxicity network based on CTD hepatotoxicity genes and its overlap with drug signatures of 4 of the top 5 predicted drugs by PharmOmics which had >50 signature genes. Phenobarbital was among the top 5 drugs but was not included in the figure due to its small DEG size. Colors of the network nodes denote the different drugs targeting the genes. The top 3 predictive subnetworks are depicted in red (D). ANOVA test followed by post-hoc analysis was used for statistics in A and C. *, **, *** indicates $p < 0.05$, $p < 0.01$ and $p < 0.001$ respectively. Boxplots show interquartile range (IQR) and median values (line inside the box). IQR was defined as between 25th (Q1) and 75th (Q3) percentile. The upper and lower bars indicate the points within Q3 + 1.5*IQR and Q1 – 1.5*IQR, respectively.

Figure 8. Utility of PharmOmics drug signatures in nephrotoxicity prediction based on matching between PharmOmics drug signatures and nephrotoxicity signatures of chemical induced acute kidney injury (AKI) or chronic kidney disease (CKD) from comparative toxicogenomics database (CTD). (A) Boxplots of Jaccard score-based nephrotoxicity ranking (left) and network-based nephrotoxicity ranking (right) by PharmOmics, based on matching with AKI (top) or CKD (bottom) nephrotoxicity genes from

CTD, across four categories of kidney histological severity defined by the independent TG-GATEs database. Network-based nephrotoxicity prediction by PharmOmics showed a positive relationship between nephrotoxicity scores by PharmOmics and kidney histology severity defined by TG-GATEs. (B) PharmOmics nephrotoxicity prediction scores based on gene signatures of higher drug doses correspond to more severe kidney injury categories defined by TG-GATES, segregated by nephrotoxic labels defined by DrugBank. (C) Boxplot of network-based nephrotoxicity scores, using CKD nephrotoxicity genes against PharmOmics drug signatures, did not show significant dose-dependent trend in non-nephrotoxic drugs or nephrotoxic drugs defined by DrugBank. The low dose treatment group for the nephrotoxic drugs did not contain drug signatures with more than 10 genes and therefore the scores were not plotted. (D) ROC curve comparing the performance of PharmOmics with other tools in predicting nephrotoxic agents in DrugBank. For PharmOmics, two sets of tests were performed, where either dose/time-segregated drug signatures or meta signatures was used. (E) Kidney nephrotoxicity network based on CTD nephrotoxicity genes and the network overlap with drug signatures of top 5 drugs predicted by PharmOmics. Colors of the network nodes denote the various drugs targeting the genes. ANOVA test with post-hoc analysis was used for statistics in A and C. *, **, *** indicates $p < 0.05$, $p < 0.01$ and $p < 0.001$ respectively. Boxplots show interquartile range (IQR) and median values (line inside the box), with IQR defined as between 25th (Q1) and 75th (Q3) percentile.

Figure 9. Cross-tissue and cross-species comparisons of drug signatures in PharmOmics. (A) Distribution of drug signature overlap percentages between tissue pairs in matching species from PharmOmics. Arrow points to the pairs of tissues for drugs with high overlap in gene signatures. (B) Upset plot of cross-tissue comparison for atorvastatin signatures genes. Y-axis indicates number of genes. (C) Upset plot of cross-tissue comparison for pathways enriched in atorvastatin signatures. Y-axis indicates number of pathways. (D) Distribution of drug signature overlap percentages between pairs of species for matching tissues from PharmOmics. Arrow points to the species pair with high gene signature overlap for a matching drug. (E) Upset plot of cross-species comparison for rosiglitazone liver gene signatures. (F) Upset plot of cross-species comparison for pathways enriched in rosiglitazone liver signatures. Pairs of tissues with shared drug signature genes or pathways are connected with black vertical lines in the bottom portion of the Upset plots.

Figures

Figure 1.

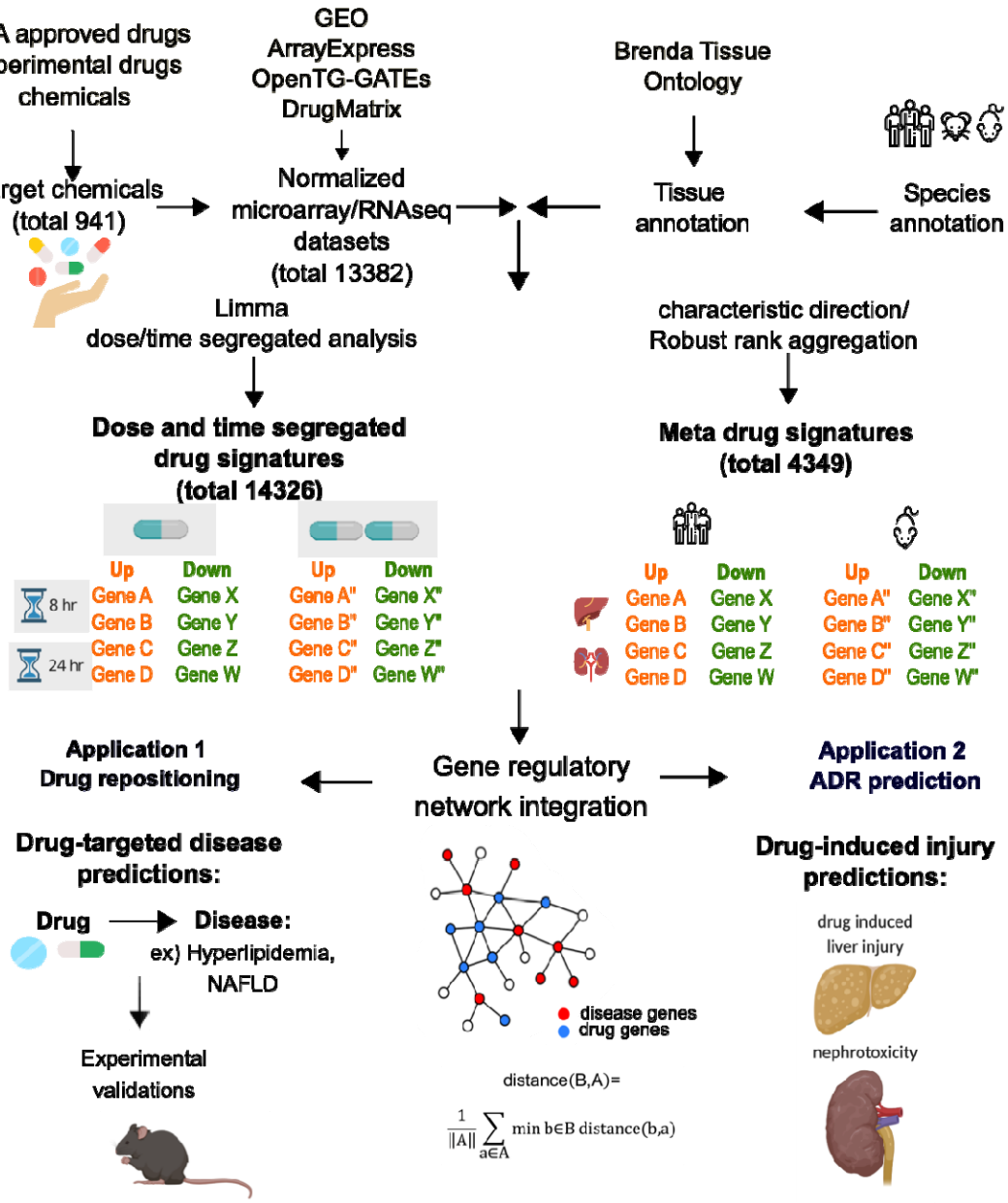

1052 **Figure 2.**

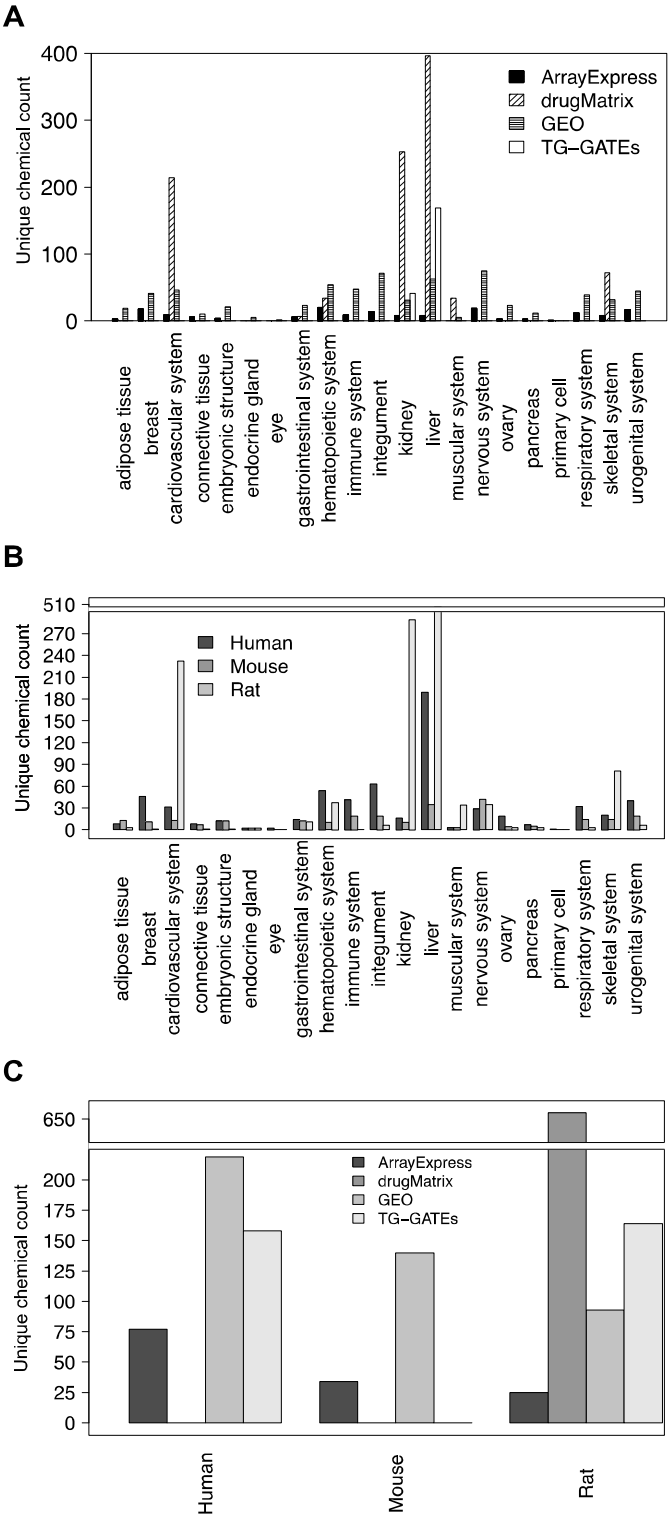

1053

1054 **Figure 3.**

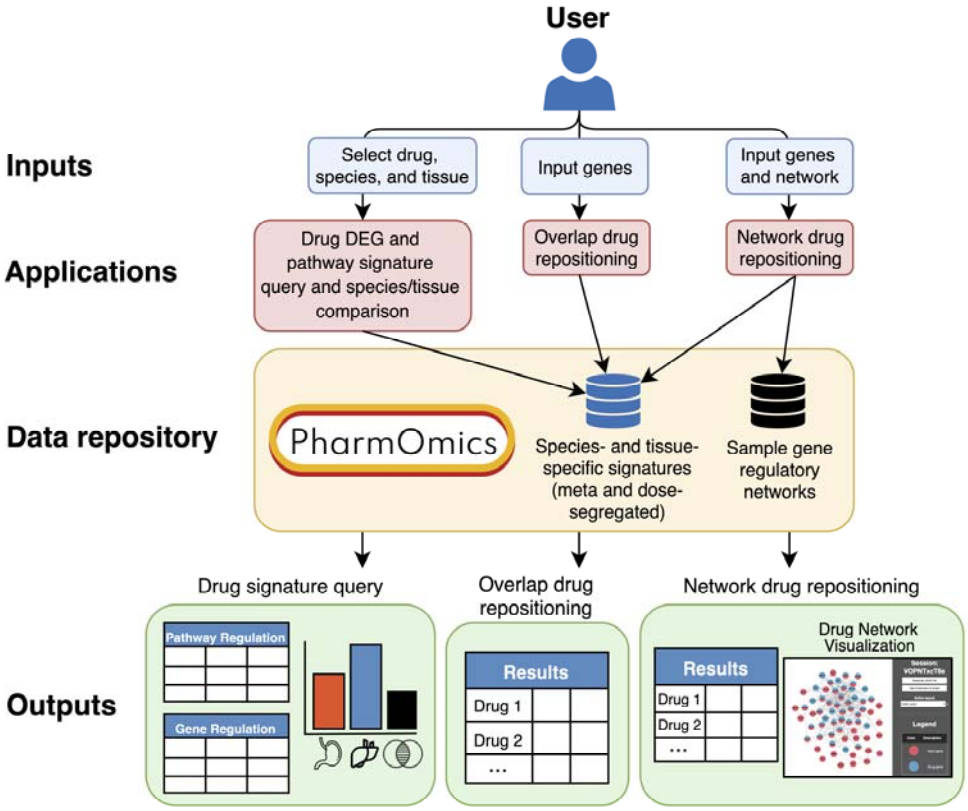

1055

1056

Figure 4.

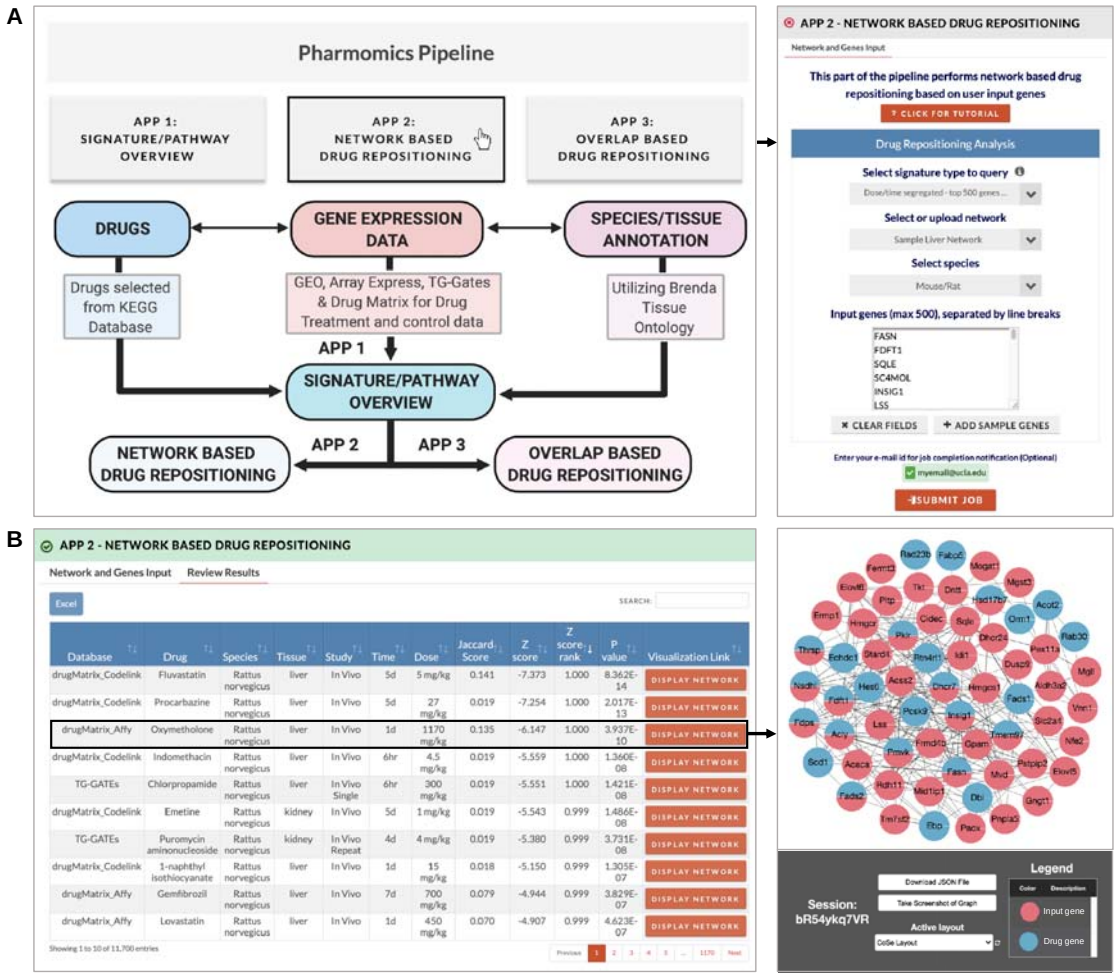

Figure 5.

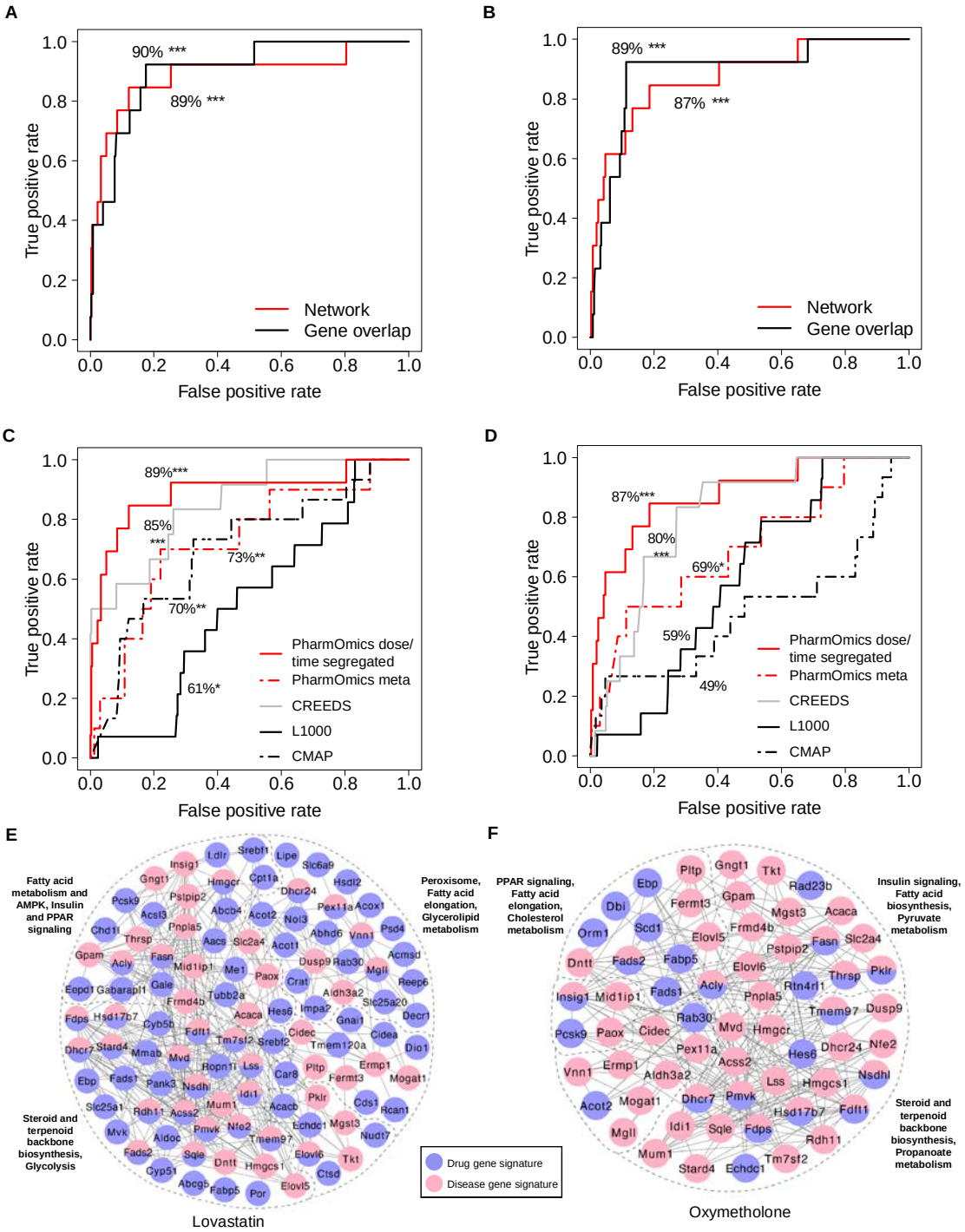

1080 **Figure 6.**

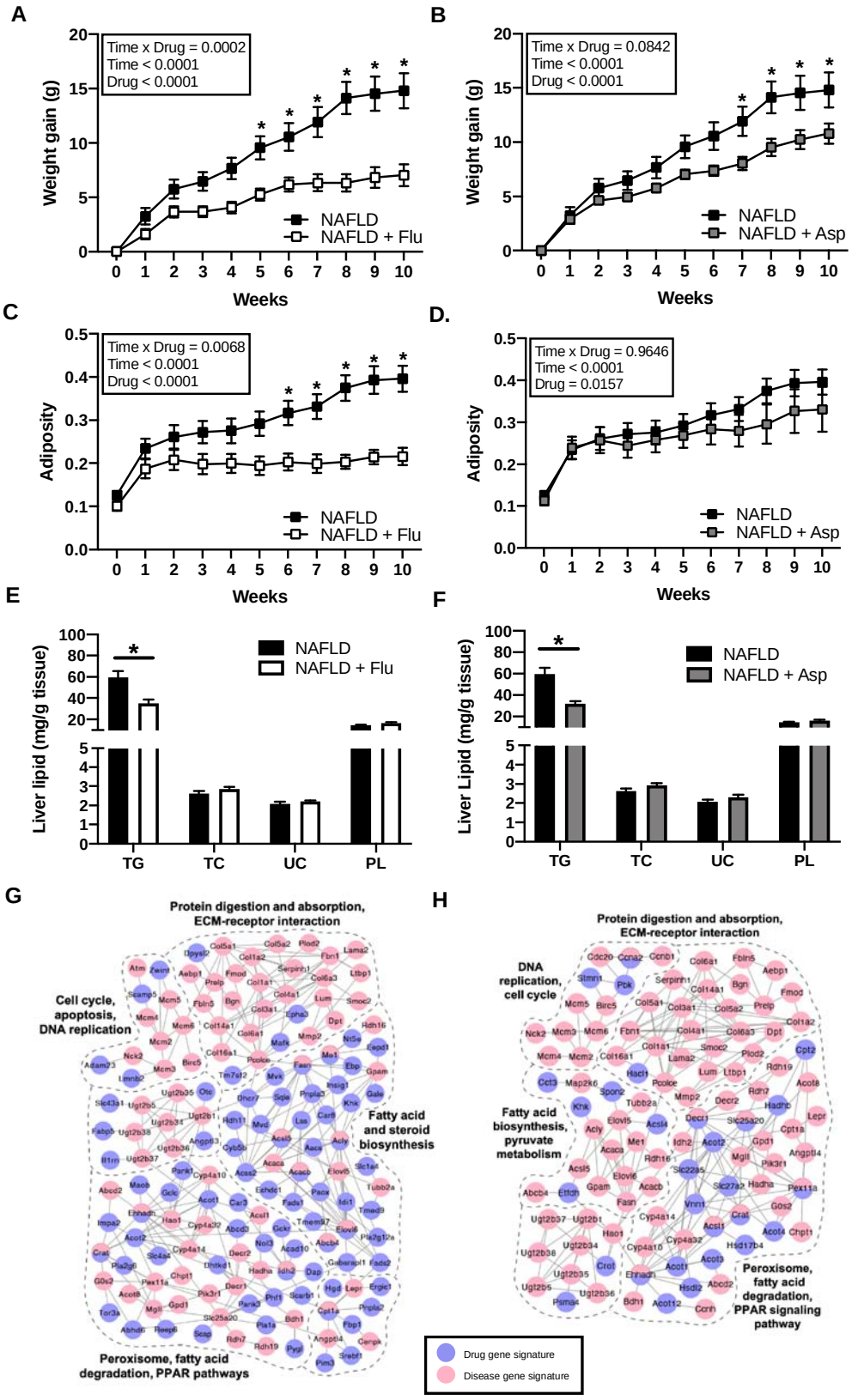

1081

1082

Figure 7.

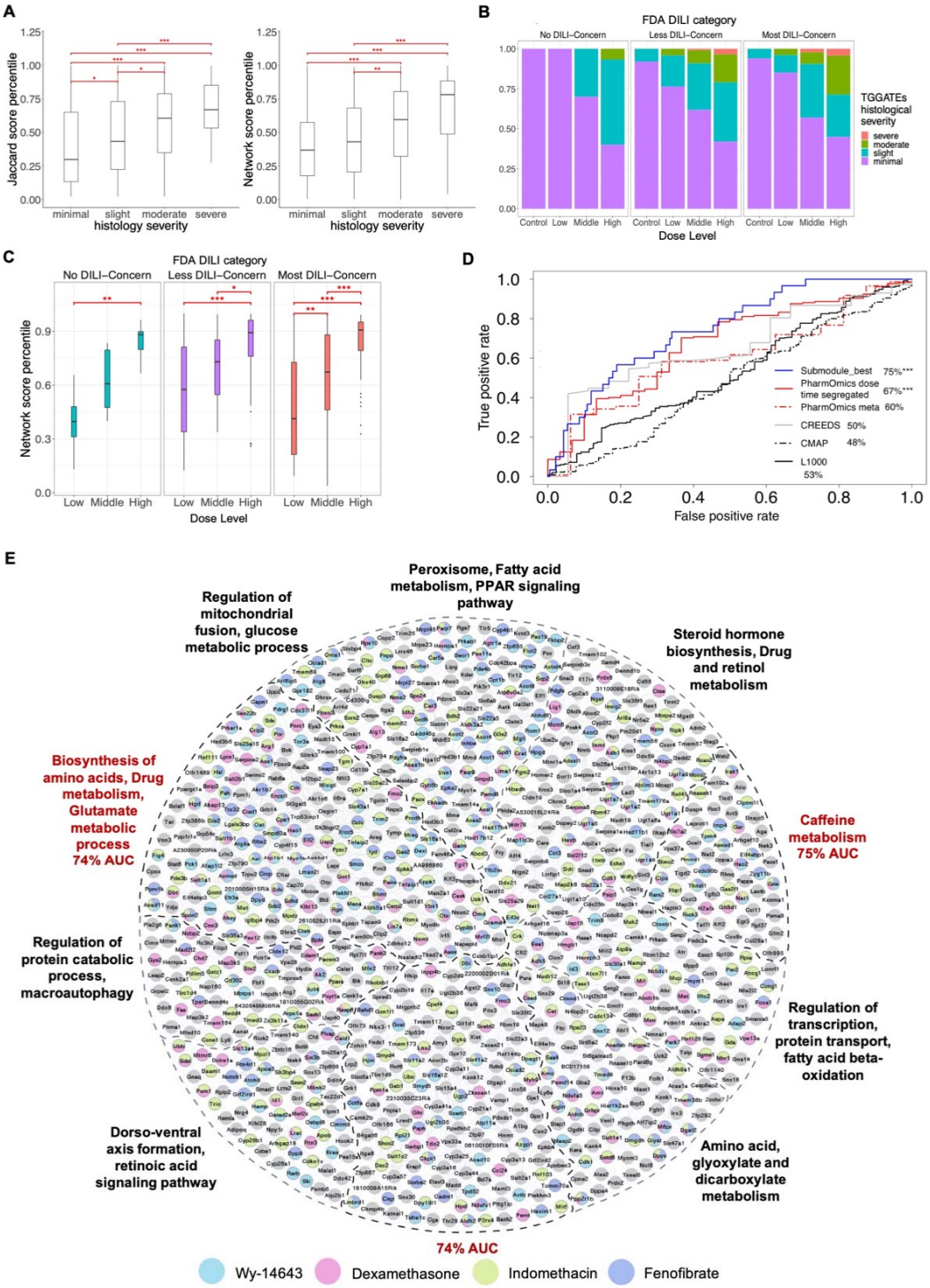

Figure 8.

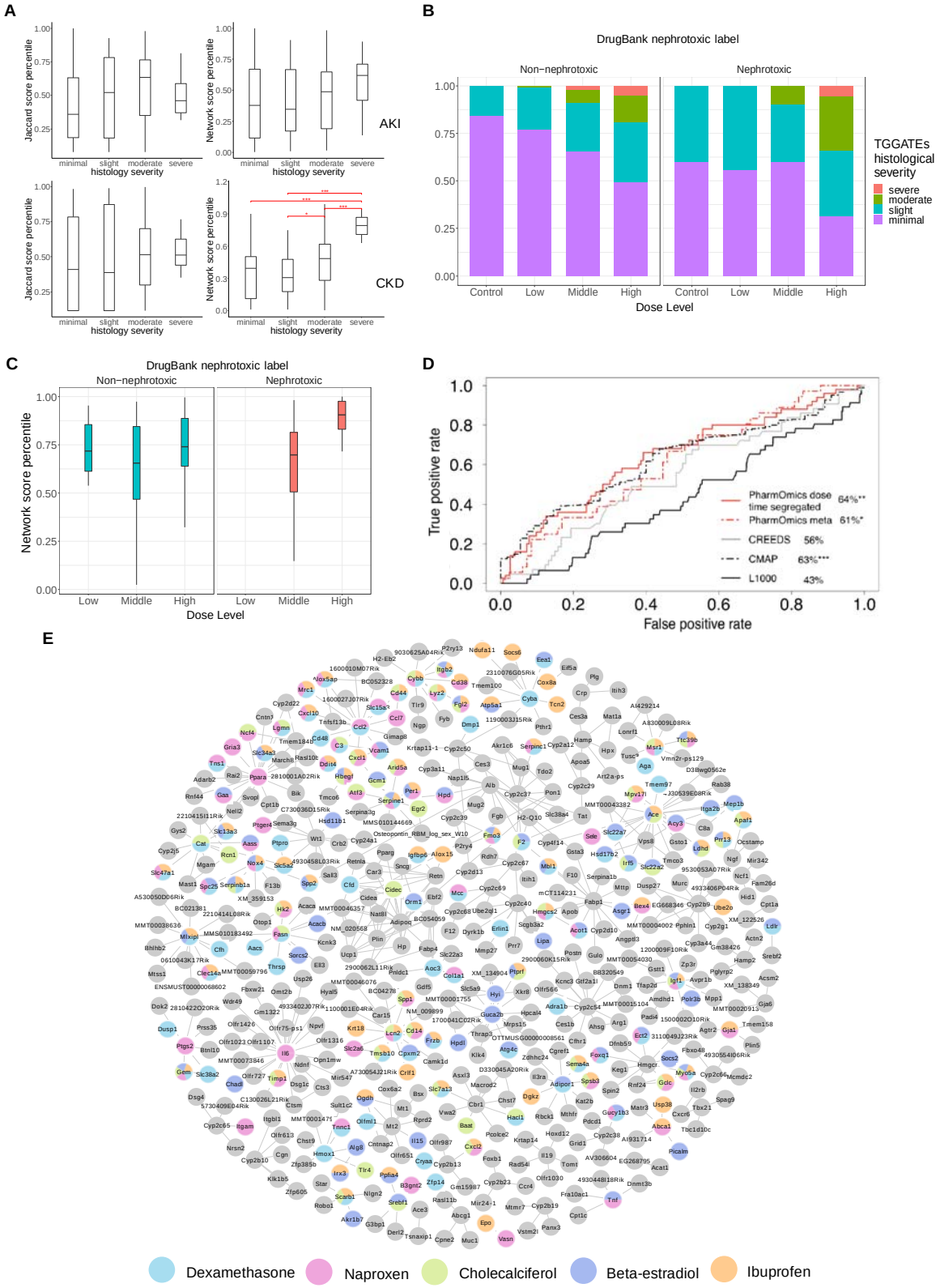

1093 **Figure 9.**

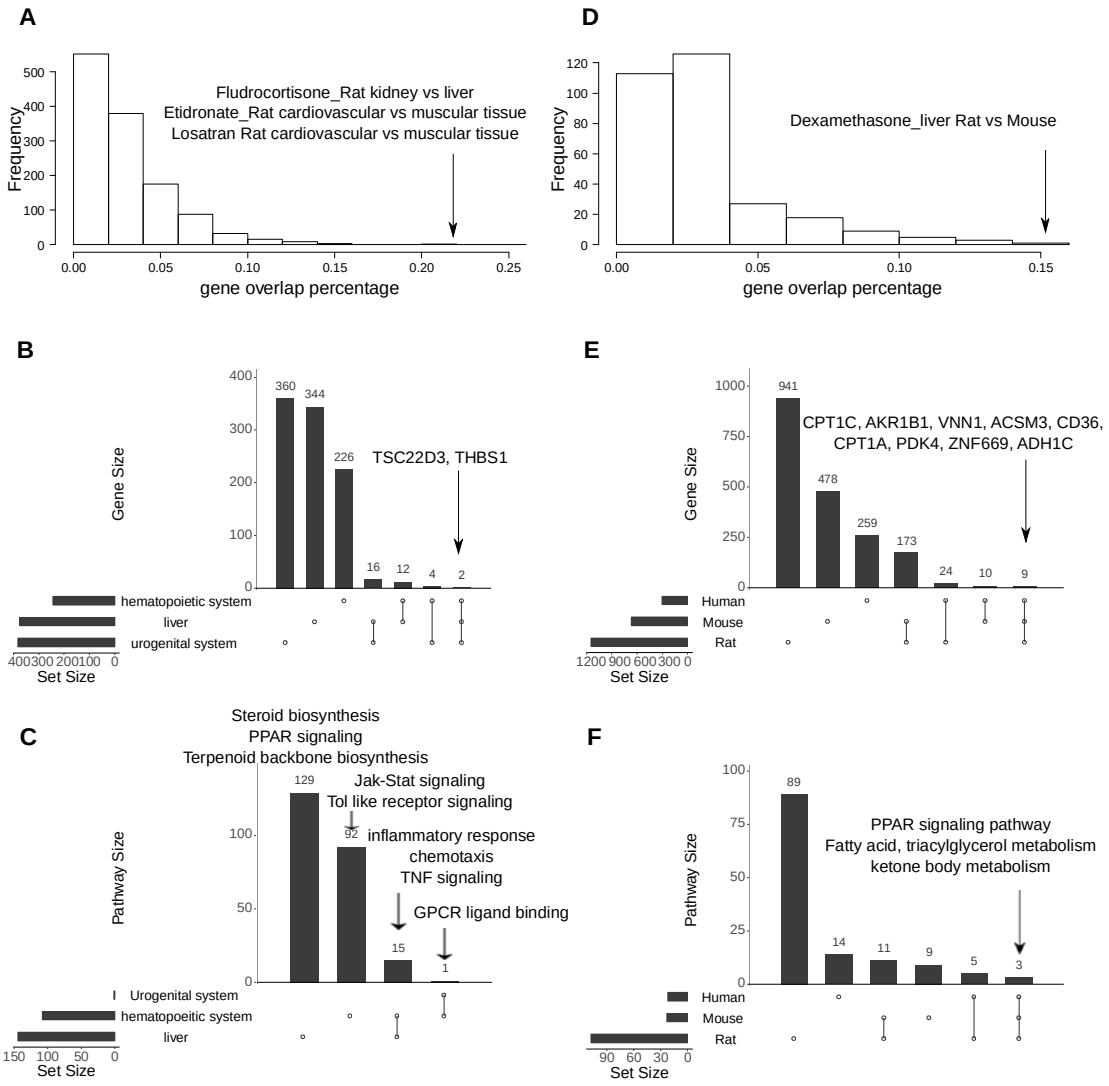

1094

FDA approved drugs
experimental drugs
chemicals

GEO
ArrayExpress
OpenTG-GATEs
DrugMatrix

Brenda Tissue
Ontology

Target chemicals
(total 941)

Normalized
microarray/RNAseq
datasets
(total 13382)

Tissue
annotation

Species
annotation

Limma
dose/time segregated analysis

characteristic direction/
Robust rank aggregation

Dose and time segregated drug signatures (total 14326)

	Up	Down	Up	Down
8 hr	Gene A	Gene X	Gene A"	Gene X"
	Gene B	Gene Y	Gene B"	Gene Y"
24 hr	Gene C	Gene Z	Gene C"	Gene Z"
	Gene D	Gene W	Gene D"	Gene W"

Meta drug signatures (total 4349)

	Up	Down	Up	Down
	Gene A	Gene X	Gene A"	Gene X"
	Gene B	Gene Y	Gene B"	Gene Y"
	Gene C	Gene Z	Gene C"	Gene Z"
	Gene D	Gene W	Gene D"	Gene W"

Application 1
Drug repositioning

Gene regulatory
network integration

Application 2
ADR prediction

Drug-targeted disease predictions:

Drug → **Disease:**
ex) Hyperlipidemia, NAFLD

Experimental validations

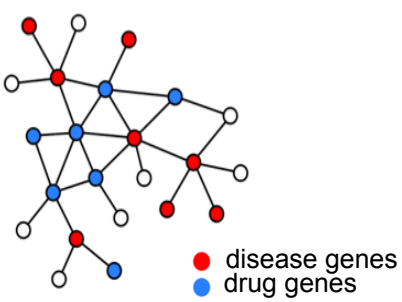

distance(B,A)=

$$\frac{1}{\|A\|}\sum_{a\in A}\min_{b\in B} \text{distance}(b,a)$$

Drug-induced injury predictions:

drug induced
liver injury

nephrotoxicity

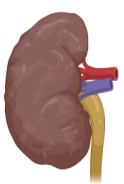

A

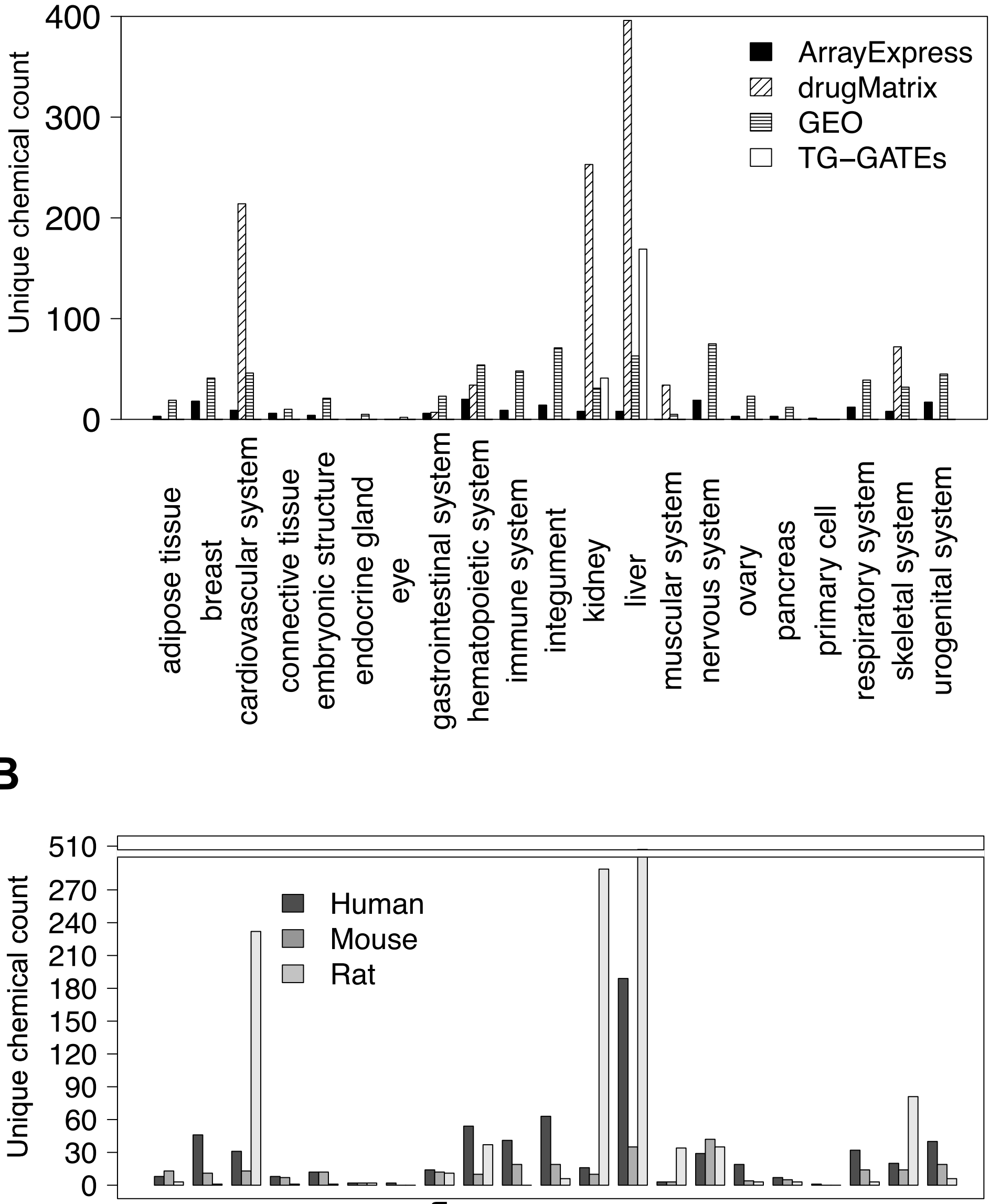

B

C

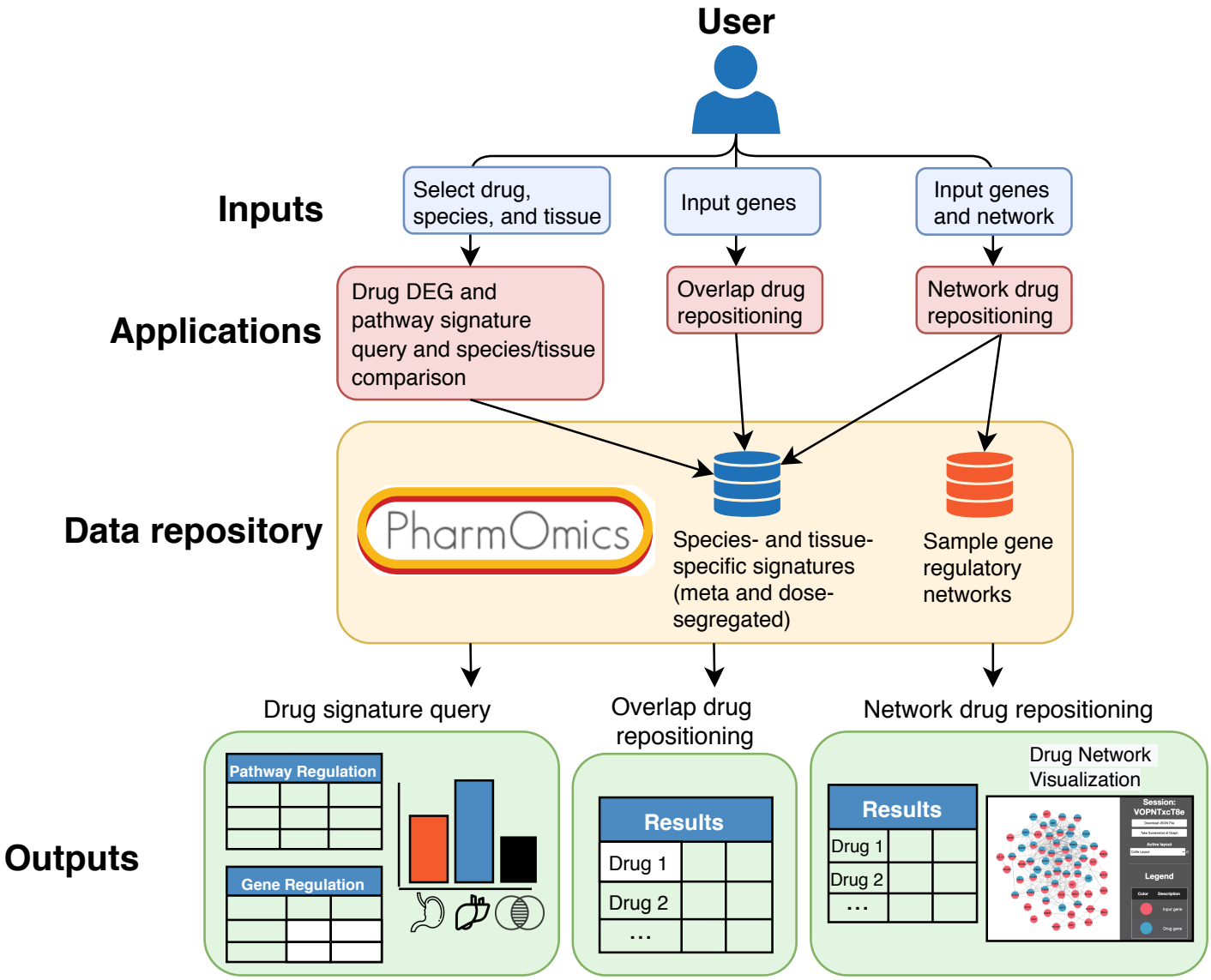

A

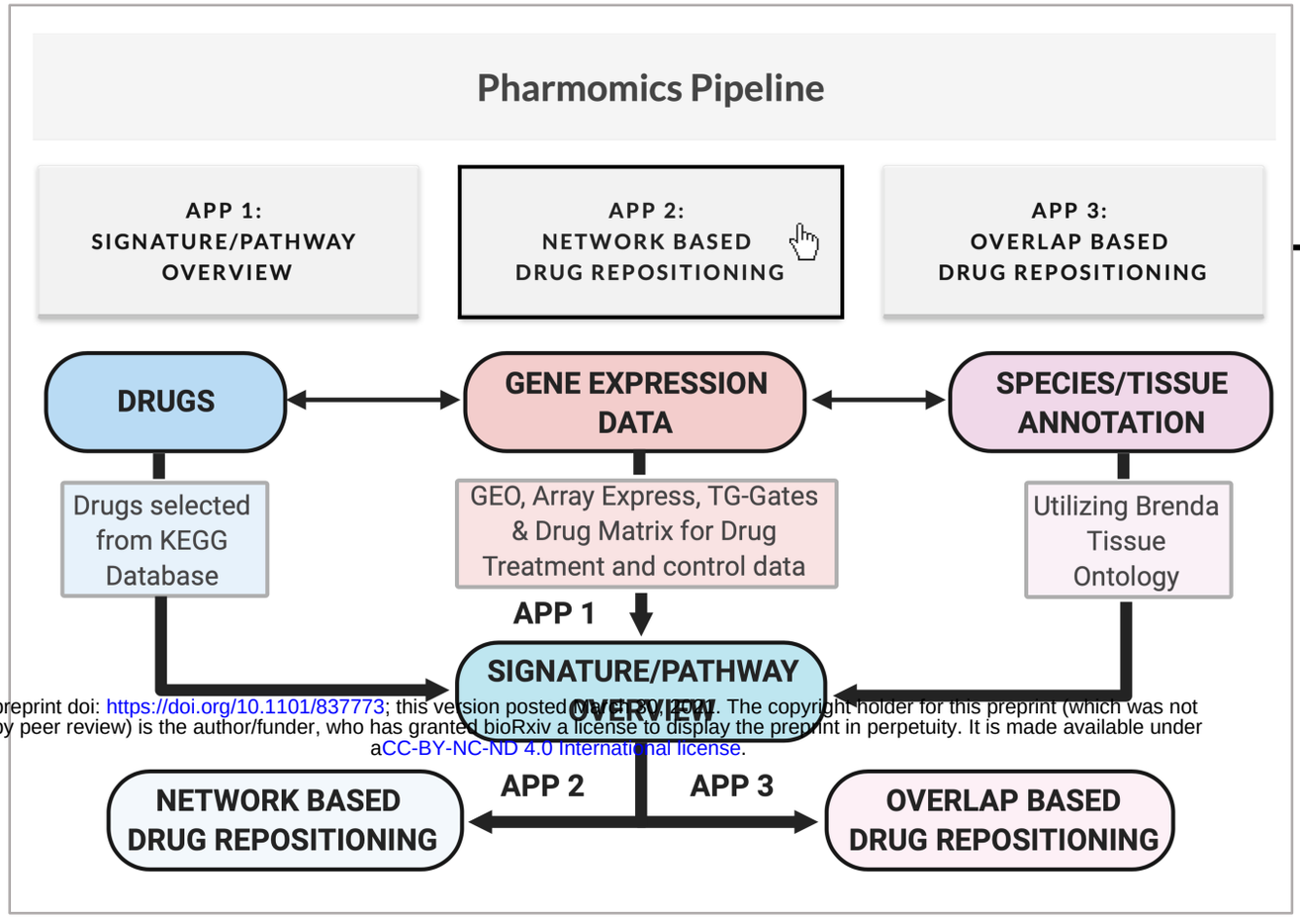

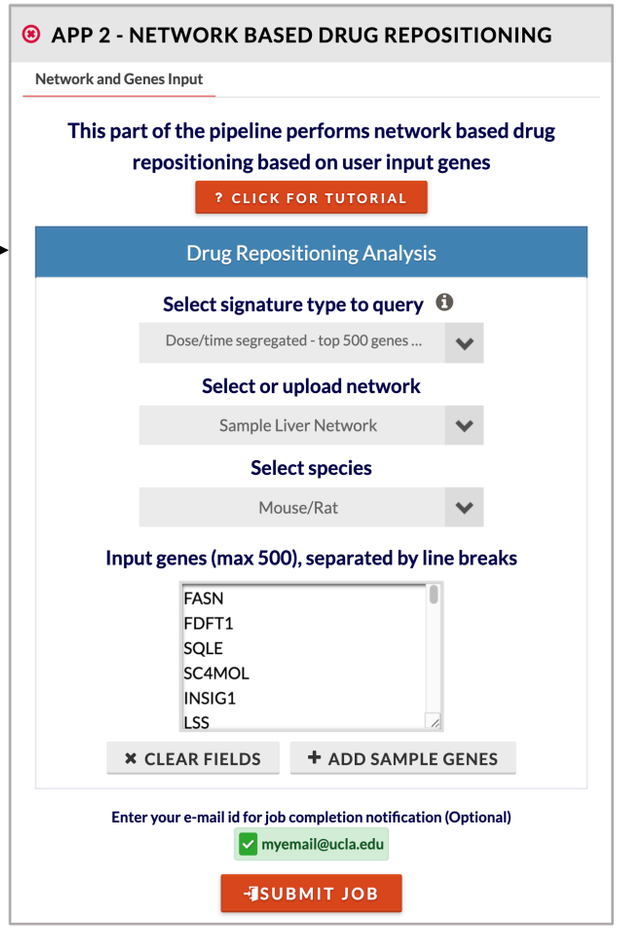

B

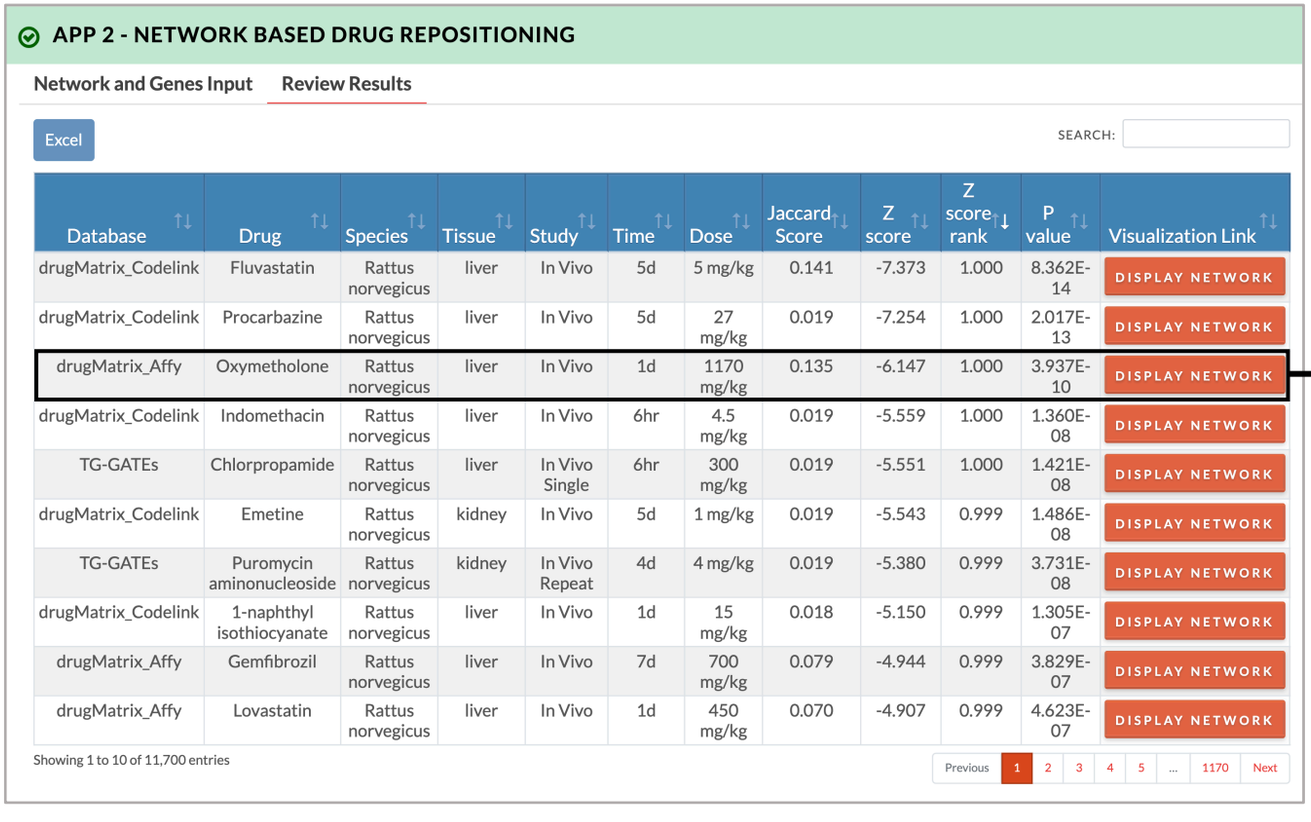

Database	Drug	Species	Tissue	Study	Time	Dose	Jaccard Score	Z score	Z score rank	P value	Visualization Link
drugMatrix_Codelink	Fluvastatin	Rattus norvegicus	liver	In Vivo	5d	5 mg/kg	0.141	-7.373	1.000	8.362E-14	DISPLAY NETWORK
drugMatrix_Codelink	Procarbazine	Rattus norvegicus	liver	In Vivo	5d	27 mg/kg	0.019	-7.254	1.000	2.017E-13	DISPLAY NETWORK
drugMatrix_Affy	Oxymetholone	Rattus norvegicus	liver	In Vivo	1d	1170 mg/kg	0.135	-6.147	1.000	3.937E-10	DISPLAY NETWORK
drugMatrix_Codelink	Indomethacin	Rattus norvegicus	liver	In Vivo	6hr	4.5 mg/kg	0.019	-5.559	1.000	1.360E-08	DISPLAY NETWORK
TG-GATEs	Chlorpropamide	Rattus norvegicus	liver	In Vivo Single	6hr	300 mg/kg	0.019	-5.551	1.000	1.421E-08	DISPLAY NETWORK
drugMatrix_Codelink	Emetine	Rattus norvegicus	kidney	In Vivo	5d	1 mg/kg	0.019	-5.543	0.999	1.486E-08	DISPLAY NETWORK
TG-GATEs	Puromycin aminonucleoside	Rattus norvegicus	kidney	In Vivo Repeat	4d	4 mg/kg	0.019	-5.380	0.999	3.731E-08	DISPLAY NETWORK
drugMatrix_Codelink	1-naphthyl isothiocyanate	Rattus norvegicus	liver	In Vivo	1d	15 mg/kg	0.018	-5.150	0.999	1.305E-07	DISPLAY NETWORK
drugMatrix_Affy	Gemfibrozil	Rattus norvegicus	liver	In Vivo	7d	700 mg/kg	0.079	-4.944	0.999	3.829E-07	DISPLAY NETWORK
drugMatrix_Affy	Lovastatin	Rattus norvegicus	liver	In Vivo	1d	450 mg/kg	0.070	-4.907	0.999	4.623E-07	DISPLAY NETWORK